CRAC channel activity in *C. elegans* is mediated by Orai1 and STIM1 homologues and is essential for ovulation and fertility

Catherine Lorin-Nebel, Juan Xing, Xiaohui Yan and Kevin Strange

Departments of Anaesthesiology, Molecular Physiology and Biophysics, and Pharmacology, Vanderbilt University Medical Center, Nashville, TN 37232, USA

The Ca^{2+} release-activated Ca^{2+} (CRAC) channel is a plasma membrane Ca^{2+} entry pathway activated by endoplasmic reticulum (ER) Ca^{2+} store depletion. STIM1 proteins function as ER Ca^{2+} sensors and regulate CRAC channel activation. Recent studies have demonstrated that CRAC channels are encoded by the human *Orai1* gene and a homologous *Drosophila* gene. *C. elegans* intestinal cells express a store-operated Ca^{2+} channel (SOCC) regulated by STIM-1. We cloned a full-length *C. elegans* cDNA that encodes a 293 amino acid protein, ORAI-1, homologous to human and *Drosophila* Orai1 proteins. ORAI-1 GFP reporters are co-expressed with STIM-1 in the gonad and intestine. Inositol 1,4,5-trisphosphate (IP_3)-dependent Ca^{2+} signalling regulates *C. elegans* gonad function, fertility and rhythmic posterior body wall muscle contraction (pBoc) required for defecation. RNA interference (RNAi) silencing of *orai-1* expression phenocopies *stim-1* knockdown and causes sterility and prevents intestinal cell SOCC activation, but has no effect on pBoc or intestinal Ca^{2+} signalling. *Orai-1* RNAi suppresses pBoc defects induced by intestinal expression of a STIM-1 Ca^{2+}-binding mutant, indicating that the proteins function in a common pathway. Co-expression of *stim-1* and *orai-1* cDNAs in HEK293 cells induces large inwardly rectifying cation currents activated by ER Ca^{2+} depletion. The properties of this current recapitulate those of the native SOCC current. We conclude that *C. elegans* expresses bona fide CRAC channels that require the function of Orai1- and STIM1-related proteins. CRAC channels thus arose very early in animal evolution. In *C. elegans*, CRAC channels do not play obligate roles in all IP_3-dependent signalling processes and ER Ca^{2+} homeostasis. Instead, we suggest that CRAC channels carry out highly specialized and cell-specific signalling roles and that they may function as a failsafe mechanism to prevent Ca^{2+} store depletion under pathophysiological and stress conditions.

(Received 13 November 2006; accepted after revision 9 January 2007; first published online 11 January 2007)
Corresponding author K. Strange: Vanderbilt University Medical Center, T-4208 Medical Center North, Nashville, TN 37232-2520, USA. Email: kevin.strange@vanderbilt.edu

Intracellular Ca^{2+} signals regulate a diverse array of physiological processes including secretion, muscle contraction, cell growth and gene expression (Berridge *et al.* 2003). Changes in cytoplasmic Ca^{2+} levels are brought about by altered flux across the plasma membrane and by release from intracellular compartments. The endoplasmic reticulum (ER) is a major cellular Ca^{2+} store. Calcium release from the ER is mediated by activation of inositol 1,4,5-trisphosphate (IP_3)-regulated Ca^{2+} channels.

Store-operated Ca^{2+} entry (SOCE) is activated by depletion of ER Ca^{2+} stores and is a widely observed mechanism of plasma membrane Ca^{2+} influx (Parekh & Penner, 1997; Venkatachalam *et al.* 2002; Parekh & Putney, 2005). Store-operated Ca^{2+} channel (SOCC) activity was first identified in 1992 by patch-clamp electrophysiology (Hoth & Penner, 1992). This SOCC was termed the Ca^{2+} release-activated Ca^{2+} (CRAC) channel and is the most extensively characterized SOCE pathway (Parekh & Penner, 1997; Parekh & Putney, 2005). The mechanisms that regulate SOCE and the molecular identity of the CRAC channel have been the subjects of intense investigation for over 15 years.

Two recent discoveries have dramatically advanced our understanding of SOCE. RNA interference (RNAi) screening in *Drosophila* S2 cells first identified stromal interaction molecule 1 (STIM1) as an essential component of CRAC activation (Roos *et al.* 2005). Studies from several laboratories have established that *Drosophila* and human

 DOI: 10.1113/jphysiol.2006.124883

STIM1 homologues function as ER Ca^{2+} sensors (Liou *et al.* 2005; Zhang *et al.* 2005; Soboloff *et al.* 2006*a*; Spassova *et al.* 2006). In response to Ca^{2+} store depletion, STIM1 undergoes redistribution from a diffuse ER localization to a punctate localization (Liou *et al.* 2005; Zhang *et al.* 2005; Baba *et al.* 2006; Wu *et al.* 2006; Xu *et al.* 2006) that corresponds to sites of ER–plasma membrane contact (Wu *et al.* 2006). This redistribution in turn activates CRAC and SOCE (Zhang *et al.* 2005; Liou *et al.* 2005; Luik *et al.* 2006; Soboloff *et al.* 2006*a* Spassova *et al.* 2006; Wu *et al.* 2006). The sites of punctate STIM1 localization also appear to be sites of localized Ca^{2+} influx and CRAC activity (Luik *et al.* 2006).

In an elegant study, Feske *et al.* (2006) used linkage analysis and a *Drosophila* S2 cell genome-wide RNAi screen to identify Orai1 as an essential component of the CRAC channel (see also Vig *et al.* 2006*b*; Zhang *et al.* 2006;). Work from several laboratories indicates that Orai1 homologues are essential components of the CRAC channel and probably function as pore subunits (Prakriya *et al.* 2006; Vig *et al.* 2006*a*; Yeromin *et al.* 2006). Co-expression of STIM1 and Orai1 homologues dramatically increases SOCE and CRAC channel activity (Mercer *et al.* 2006; Peinelt *et al.* 2006; Prakriya *et al.* 2006; Soboloff *et al.* 2006*b* Vig *et al.* 2006*a*; Yeromin *et al.* 2006;). During SOCE/CRAC channel activation, Orai1 redistributes from a diffuse localization pattern in the plasma membrane and colocalizes with STIM1 puncta (Luik *et al.* 2006; Xu *et al.* 2006). Co-immunoprecipitation studies suggest that STIM1 and Orai1 homologues bind to each other directly or through intermediary proteins (Vig *et al.* 2006*a*; Yeromin *et al.* 2006). Together, these observations have led to the hypothesis that redistribution and subsequent co-association of STIM1 and Orai1 homologues in response to ER Ca^{2+} depletion activates CRAC channels and SOCE.

Depletion of ER Ca^{2+} stores in *C. elegans* intestinal cells activates a SOCC current with many of the same biophysical properties as I_{CRAC} (Estevez *et al.* 2003). We demonstrated recently that a single STIM1 homologue encoding gene *stim-1* is present in the worm genome. Green fluorescent protein (GFP)-tagged STIM-1 is expressed in several cell types including cells of the intestine and gonad (Yan *et al.* 2006). IP_3-dependent Ca^{2+} signals control the contractile properties of gonad cells required for ovulation in *C. elegans* (Clandinin *et al.* 1998; Bui & Sternberg, 2002; Kariya *et al.* 2004; Yin *et al.* 2004). Oscillatory Ca^{2+} signals with a period of ~50 s occur in the worm intestine and trigger rhythmic posterior body wall muscle contraction (pBoc) required for defecation (Dal Santo *et al.* 1999; Espelt *et al.* 2005; Teramoto & Iwasaki, 2006). SOCE is thought to be essential for maintenance of ER Ca^{2+} stores and intracellular Ca^{2+} signalling (Parekh & Penner, 1997; Venkatachalam *et al.* 2002; Parekh & Putney, 2005). RNA interference silencing of *C. elegans* *stim-1* expression causes complete sterility and prevents activation of intestinal SOCCs but surprisingly has no effect on pBoc or intestinal Ca^{2+} oscillations (Yan *et al.* 2006). These and other findings suggest that SOCE is not essential for certain oscillatory Ca^{2+} signalling processes or for maintenance of store Ca^{2+} levels in *C. elegans*, and raise important questions regarding the function of SOCE and SOCCs under normal and pathophysiological conditions (Yan *et al.* 2006).

In an effort to further exploit *C. elegans* as a model system for characterizing SOCE, we conducted a BLAST search and identified a single gene (*orai-1*) that encodes a 293 amino acid protein with 55% overall similarity to human Orai1. ORAI-1::GFP and STIM-1::GFP reporters are co-expressed in specific cell and tissue types, and knockdown of *orai-1* expression phenocopies the effect of *stim-1* RNAi. *Orai-1* RNAi suppresses pBoc defects induced by expression of a STIM-1 EF hand mutant in the worm intestine, indicating that the two proteins function together. Furthermore, co-expression of *stim-1* and *orai-1* cDNAs in HEK293 cells induces large inwardly rectifying cation currents activated by ER Ca^{2+} depletion. Our results demonstrate that *C. elegans* expresses bona fide CRAC channels and that, as in *Drosophila* and mammals, channel activity requires the function of STIM1 and Orai1-related proteins. STIM1 and Orai1 homologues have not yet been detected in plants and single-celled organisms, suggesting that CRAC channels arose very early in animal evolution and that they carry out conserved physiological functions. The present work and our previous studies (Estevez *et al.* 2003; Yan *et al.* 2006) underscore the utility of *C. elegans* as a model system for developing a detailed molecular and integrative physiological understanding of CRAC channel function and regulation.

Methods

Celegans strains

Nematodes were cultured using standard methods (Brenner, 1974). Wild-type worms were the Bristol N2 strain. The following mutant/transgenic strains were used: NL2098 [*rrf-1(pk1417)*], VP303 [*rde-1(ne219); kbEx200*] (Espelt *et al.* 2005), VP506 [*kbIs15(Pstim-1::STIM-1(D55A; D57A)::GFP)*] (Yan *et al.* 2006) and BC10427 [*sEx10427(Porai-1::GFP)*]. All worm strains were grown at 16–25°C.

Analysis of sheath cell contraction and ovulation

Young adult worms that had undergone no more than one ovulation attempt were anaesthetized for 30–40 mins in M9 solution containing 0.1% tricaine and 0.01% tetramisole, mounted onto 2% agarose pads (McCarter *et al.* 1999) and then imaged at room temperature (22–23°C) by differential interference

contrast (DIC) microscopy using a Nikon (Melville, NY, USA) Eclipse TE2000 inverted microscope and a Superfluor 40×/1.3 NA oil immersion objective lens. Images were recorded at 30 frames s^{-1} on videotape using a DAGE-MTI (Michigan City, Indiana) CCD100 camera and analysed offline. Sheath contractions were counted in 1 min intervals.

Measurement of brood size

Brood size was quantified at 25°C by transferring single L4 larvae to new growth plates daily for 4 days. The number of progeny on each plate was counted 24–36 h after eggs hatched.

Characterization of pBoc cycle

Posterior body wall muscle contraction (pBoc) was monitored at room temperature (21–22°C) in 2-day-old adult worms. A minimum of 10 pBoc cycles were measured in each animal. Worms were imaged using a Zeiss Stemi SV11 M^2BIO stereo dissecting microscope (Kramer Scientific Corp., Valley Cottage, NY, USA), equipped with a DAGE-MTI (Michigan City, IN, USA) DC2000 CCD camera. pBoc rhythmicity in individual worms was assessed by calculating the coefficient of variance (CV), which is the standard deviation expressed as a percentage of the mean.

Dissection and fluorescence imaging of intestines

Calcium oscillations were measured in isolated intestines as previously described (Espelt *et al.* 2005). Briefly, worms were placed in control saline (mM: 137 NaCl, 5 KCl, 1 $MgCl_2$, 1 $MgSO_4$, 0.5 $CaCl_2$, 10 Hepes, 5 Glucose, 2 L-asparagine, 0.5 L-cysteine, 2 L-glutamine, 0.5 L-methionine, 1.6 L-tyrosine, 27 sucrose, pH 7.3, 340 mosol l^{-1}) and cut behind the pharynx using a 26-gauge needle. The hydrostatic pressure in the worm spontaneously extruded the intestine, which remained attached to the rectum and the posterior end of the animal. Isolated intestines were incubated for 10 min in bath saline containing 5 μM fluo-4 AM and 1% bovine serum albumin (BSA). Imaging was performed at room temperature (21–22°C) using a Nikon TE2000 inverted microscope, a Superfluor 40×/1.3 NA oil objective lens, a Photometrics Cascade 512B cooled CCD camera (Roper Industries, Duluth, GA, USA) and MetaFluor software (Universal Imaging Corporation, Downingtown, PA, USA). Fluo-4 was excited using a 490–500 BP filter and a 523–547 BP filter was used to detect fluorescence emission. Changes in fluo-4 intensity were quantified using region-of-interest selection and MetaFluor software (Universal Imaging Corporation, Downingtown, PA, USA).

Calcium oscillation period, rise time (RT) and fall time (FT) were quantified as previously described (Prakash *et al.* 1997; Espelt *et al.* 2005). Fluorescence images were typically acquired at 0.2 Hz, to avoid photobleaching and damage to the intestinal epithelium. However, when Ca^{2+} spike period, rise and fall times were quantified, images were acquired at 1–3 Hz.

C. elegans embryonic cell culture and patch-clamp electrophysiology

Embryo cells were isolated from *rde-1(ne219);kbEx200* worms and cultured on 12 mm diameter acid-washed glass coverslips using methods previously described (Christensen *et al.* 2002; Estevez *et al.* 2003). Intestinal cells were identified in culture by their shape and the presence of highly refractile cytoplasmic granules (Fukushige *et al.* 1998; Estevez *et al.* 2003).

Coverslips with cultured embryo cells were placed in the bottom of a bath chamber (model R-26G; Warner Instrument Corp., Hamden, C, USA) that was mounted onto the stage of a Nikon TE2000 inverted microscope. Cells were visualized by video-enhanced DIC microscopy. Patch electrodes were pulled from soft glass capillary tubes (PG10165-4, World Precision Instruments, Sarasota, F, USA) that had been silanized with dimethyl-dichloro silane. Pipette resistance was 4–7 MΩ. Bath and pipette solutions contained (mM): 145 NaCl, 20 $CaCl_2$, 10 Hepes, 20 Glucose, pH 7.2 (adjusted with NaOH), 345–350 mosmol l^{-1} and 147 sodium gluconate (Na-gluconate), 0.6 $CaCl_2$, 6 $MgCl_2$, 10 BAPTA, 10 Hepes, 10 μM IP_3, pH 7.2 (adjusted with CsOH), 330 mosmol l^{-1}, respectively.

Whole-cell currents were recorded using an Axopatch 200B (Axon Instruments, Foster City, CA, USA) patch-clamp amplifier. Command voltage generation, data digitization, and data analysis were carried out on a 1.6 GHz Pentium computer (Dimension 4400; Dell Computer Corp) using a Digidata 1322A AD/DA interface with pClamp 10 and Clampfit 10 software (Axon Instruments). Electrical connections to the amplifier were made using Ag/AgCl wires and 3 M KCl/agar bridges. Leak current was defined as the current observed immediately after obtaining whole-cell access, and was subtracted from all subsequent current records obtained in the cell.

Heterologous expression of ORAI-1 and STIM-1

HEK293 (human embryonic kidney) cells were cultured in 35 mm diameter tissue culture plates in Eagle's minimal essential medium (MEM; Invitrogen, Carlsbad, CA, USA), containing 10% fetal bovine serum (Invitrogen), non-essential amino acids, sodium pyruvate, 50 μ ml^{-1} penicillin and 50 μg ml^{-1} streptomycin. After reaching

approximately 50% confluency, cells were transfected using FuGENE 6 Transfection Reagent (Roche, Indianapolis, IN, USA), with 1 or 2 μg GFP, 1 μg STIM-1 and/or 1 μg ORAI-1 cDNA ligated into pcDNA3.1/V5-His-TOPO (Invitrogen). The total amount of cDNA transfected into cells for all experiments was 3 μg.

HEK293 cells were incubated with cDNAs for ~24 h. Two hours before initiating electrophysiological experiments, transfected cells were dissociated by exposure to 0.25% trypsin containing 1 mM EDTA (Gibco) for 45 s, and then plated onto poly L-lysine-coated coverslips. Plated coverslips were placed in a bath chamber mounted onto the stage of an inverted microscope. Cells were visualized by fluorescence and differential interference contrast microscopy.

Transfected cells were identified by GFP fluorescence and patch clamped using methods similar to those described above for embryo cells. Leak current was defined as the current observed immediately after obtaining whole-cell access, and was subtracted from all subsequent current records obtained in the cell. Standard bath and pipette solutions contained (mM): 135 NaCl, 1.2 $MgCl_2$, 10 $CaCl_2$, 10 Hepes and 10 glucose (pH 7.4, 300 mosmol l^{-1}), and 110 NMDG-gluconate or Na-gluconate, 8 $MgCl_2$, 0.6 $CaCl_2$, 10 Hepes, 10 BAPTA and 10 μM IP_3 (pH 7.2, 280 mosmol l^{-1}), respectively. Divalent cation-free bath solution contained (mM): 145 NaCl, 10 Hepes, 10 glucose and 1 EDTA (pH 7.4, 300 mosmol l^{-1}). To prevent ER Ca^{2+} store depletion, a pipette solution containing (mM): 105 NMDG-gluconate, 8 $MgCl_2$, 5 $CaCl_2$, 10 BAPTA, 10 Hepes and 2 ATP (pH 7.2, 280 mosmol l^{-1}) was used.

Relative Cs^+ permeability was determined using the Goldman–Hodgkin–Katz equation, and change in reversal potential (E_{rev}) induced by replacing NaCl in the divalent cation-free bath with CsCl. Changes in liquid junction potential induced by this ion substitution were measured directly using a free-flowing 3 M KCl electrode. Reversal potentials were corrected for these changes.

Construction of transgenes and transgenic worms

A full-length *orai-1* cDNA was cloned from a *C. elegans* cDNA library by PCR amplification. Primers were designed based on the predicted WormBase sequence of C09F5.2. Full-length translational GFP and DsRed reporters for ORAI-1 and STIM-1 (Yan *et al.* 2006), respectively, were generated using a PCR fusion-based method (Hobert, 2002) and inserted into Fire vector pPD95.77 (GFP) or a modified pPD95.77, pXHY2006.1, in which GFP was replaced with DsRed. GFP or DsRed were fused to the C-termini of the proteins. Expression of ORAI-1::GFP and STIM-1::DsRed were driven by 4 kb and 1.9 kb, respectively, of promoter sequence upstream of the *orai-1* and *stim-1* start codons. Promoter sequences were amplified by PCR from *C. elegans* N2 genomic DNA. Transgenic worms were generated by injecting wild-type worms with DNA as described by Mello *et al.* (1991). *Rol-6* was used as a transformation marker, and co-injected with STIM-1 and ORAI-1 DNA.

An integrated line of worms expressing ORAI-1::GFP and STIM-1::DsRed was generated by exposing 50 P0 *Porai-1::ORAI-1::GFP;Pstim-1::STIM-1::DsRed;rol-6(su1006)* transgenic L4 animals to a dose of 30 000 μJ cm^{-2} of UV light that was generated with a UV crosslinker (Hoefer Scientific Instruments, San Francisco, CA, USA). Five hundred F1 roller offspring were isolated, and then two F2 roller offspring from each F1 worm were isolated. A single integrated line, *KbIs18 (Porai-1::ORAI-1::GFP;Pstim-1::STIM-1::DsRed; rol-6(su1006))*, was then isolated that segregated 100% GFP, DsRed and *rol-6*-positive animals.

RNA interference

RNA interference was induced by feeding worms bacteria producing double-stranded RNA (dsRNA) (e.g. Kamath *et al.* 2000; Rual *et al.* 2004). The *orai-1* RNAi bacterial strain was obtained from the ORF-RNAi feeding library (Open Biosystems, Huntsville, AL, USA). GFP dsRNA-producing bacteria were engineered as previously described (Yin *et al.* 2004). The ORF-RNAi *orai-1* bacterial feeding strain targeted the entire open reading frame of ORAI-1. BLAST searches of *C. elegans* genomic and EST databases failed to identify genes with nucleotide sequence homology to the *orai-1* open reading frame, indicating that off-target effects of RNAi are unlikely. Bacterial strains were streaked to single colonies on agar plates containing 50 μg ml^{-1} ampicillin and 12.5 μg ml^{-1} tetracycline. Single colonies were used to inoculate LB media containing 50 μg ml^{-1} ampicillin, and cultures were grown at 37°C for 16–18 h with shaking. Four hundred microlitres of each bacterial culture were seeded onto 60 mm nematode growth medium (NGM) agar plates containing 1 mM IPTG and 50 μg ml^{-1} ampicillin. After seeding, plates were left at room temperature overnight. The effectiveness of *orai-1* silencing was assessed by measuring whole-worm fluorescence in animals expressing ORAI-1::GFP, using a COPAS Biosort (Union Biometrica, Somerville, MA, USA).

For cell culture studies, an *orai-1* DNA template was generated by PCR from the ORF-RNAi clone using T7 primers. dsRNA was synthesized from the DNA template by T7 polymerase reactions (MEGAscript kit, Ambion, Inc., Austin, TX, USA).

Isolated embryo cells were seeded onto glass coverslips in individual wells of four-well culture plates (Nalge Nunc International, Naperville, IL, USA). The cells were

incubated initially with 100 μl of L-15 cell culture medium (Life Technologies, Grand Island, NY, USA) containing 15 μg ml^{-1} of *orai-1* dsRNA. After 2 h, the culture medium volume was increased to 300 μl and the final dsRNA concentration diluted to 5 μg ml^{-1}. An additional 100 μl of L-15 containing 5 μg ml^{-1} *orai-1* dsRNA was added on the second and third day of culture. Cells were patched clamp 2–3 days after seeding.

Microscopy

Fluorescence and DIC micrographs were obtained using a Zeiss M^{2}BIO stereo dissecting microscope and DAGE-MTI DC2000 CCD camera or a Nikon TE2000 inverted microscope and a Micromax CCD-1300 camera (Princeton Instruments, Tucson, AZ, USA). Confocal imaging was performed using an LSM510 confocal microscope (Carl Zeiss MicroImaging, Inc., Thornwood, NY, USA).

Statistical analysis

Data are presented as means ± S.E.M. Statistical significance was determined using Student's two-tailed *t* test for unpaired means. When comparing three or more groups, statistical significance was determined by one-way analysis of variance. *P* values of $\leq$0.05 were taken to indicate statistical significance.

Results

A single Orai homologue is present in the *C. elegans* genome

BLAST searches of genomic and EST databases demonstrated that a single predicted Orai homologue (sequence name C09F5.2; accession number U22832) is present in the *C. elegans* genome. We cloned a full-length C09F5.2 cDNA that encoded a 293 amino acid protein, ORAI-1, with a sequence identical to that predicted by WormBase.

Sequence analysis indicated that ORAI-1 shares 34–38% and 54–59% amino acid identity and similarity, respectively, with *Drosophila* Orai and human Orai1, Orai2 and Orai3. Alignment of the amino acid sequences of ORAI-1, *Drosophila* Orai, and the three human Orai homologues is shown in Fig. 1. The four predicted transmembrane (TM) domains show strong conservation of primary structure in all five proteins. In addition, the predicted intracellular loop between TM2 and TM3 is highly conserved. Glutamate residues located in TM1 and TM3 have recently been shown to play key roles in controlling CRAC channel ion selectivity (Prakriya & Lewis, 2006; Vig *et al.* 2006*a*; Yeromin *et al.* 2006) and are fully conserved in worm, fly and human Orai homologues (arrowheads, Fig. 1). Mutation of an arginine residue at the beginning of TM1 in human Orai1 is responsible for the loss of CRAC channel activity in lymphocytes of a subset of severe combined immuno deficiency (SCID) patients

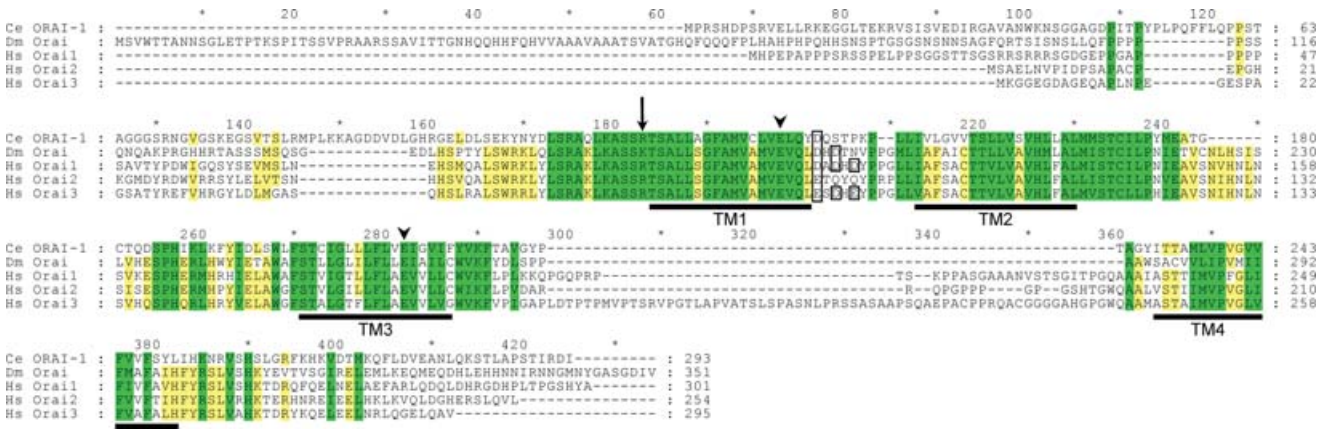

Figure 1. Amino acid sequence alignment of *C. elegans* (Ce) ORAI-1 with *Drosophila* (Dm) Orai and human (Hs) Orai1, Orai2 and Orai3
Yellow and green shading indicates sequence identity and conserved amino acid substitutions, respectively. Transmembrane (TM) domains of ORAI-1 predicted by TMpred (www.ch.embnet.org/software/TMPRED_form.html#) are underlined in black. A conserved arginine residue mutated in SCID patients lacking lymphocyte CRAC channel activity (Feske *et al.* 2006) is denoted by the arrow. Conserved glutamate residues located in TM1 and TM3 that contribute to channel ionic selectivity (Prakriya & Lewis, 2006; Vig *et al.* 2006*a*; Yeromin *et al.* 2006) are denoted by arrowheads. Alignment was performed using Vector NTI software (InforMax, Bethesda, MD, USA). Percentage identity and similarity of *C. elegans* ORAI-1 to *Drosophila* Orai, human Orai1, human Orai2 and human Orai3 were 34% and 55%, 34% and 54%, 38% and 59%, and 35% and 59%, respectively. Acidic residues in the extracellular loop between TM1 and TM2 are outlined in black. In *Drosophila* Orai (Yeromin *et al.* 2006) and human Orai1 (Vig *et al.* 2006*a*), these residues may function to attract polyvalent cations towards the channel pore and control channel selectivity.

(Feske *et al.* 2006). This residue is conserved in worm and human Orai proteins and exhibits a conserved substitution with lysine in fly Orai (arrow, Fig. 1).

The extracellular loop located between TM1 and TM2 contains two acidic amino acid residues in *Drosophila* Orai and three acidic residues in human Orai1 and Orai3 (see black boxes, Fig. 1). Mutagenesis studies on *Drosophila* Orai (Yeromin *et al.* 2006) and human Orai1 (Vig *et al.* 2006*a*) suggest that these residues may function to attract polyvalent cations towards the channel pore and control channel selectivity. Interestingly, only a single acidic residue is present in this region of *C. elegans* ORAI-1 and human Orai2 (Fig. 1), suggesting that these channels may exhibit selectivity properties distinct from other Orai homologues.

ORAI-1 is expressed in functionally diverse tissue types

To identify cells in which ORAI-1 is expressed, we generated transgenic worms expressing full-length ORAI-1 fused to GFP. Expression was driven by 4 kb of the *orai-1* promoter located immediately upstream of the start codon. Prominent expression of ORAI-1::GFP was detected in the spermatheca, intestine and hypodermis (Fig. 2*A* and *B*). Intestinal expression appeared to be localized to both apical and basolateral membrane regions (Fig. 2*A*).

The spermatheca is an accordian-like tube comprised of 24 cells. Apical and basal surfaces of the spermatheca are collapsed and highly folded in the absence of an oocyte. The circumferential ORAI-1::GFP localization pattern shown in Fig. 2*B* is consistent with expression in the basal plasma membrane. Non-circumferential localization is probably due to membrane folding and/or expression at lateral cell borders. The complicated morphology of the spermatheca precluded definitive localization of ORAI-1::GFP to the apical cell membrane.

In the intact animal, it was unclear whether gonadal sheath cells expressed ORAI-1::GFP, due to the intense fluorescence from the intestine and spermatheca. To examine sheath cell expression further, we imaged gonads

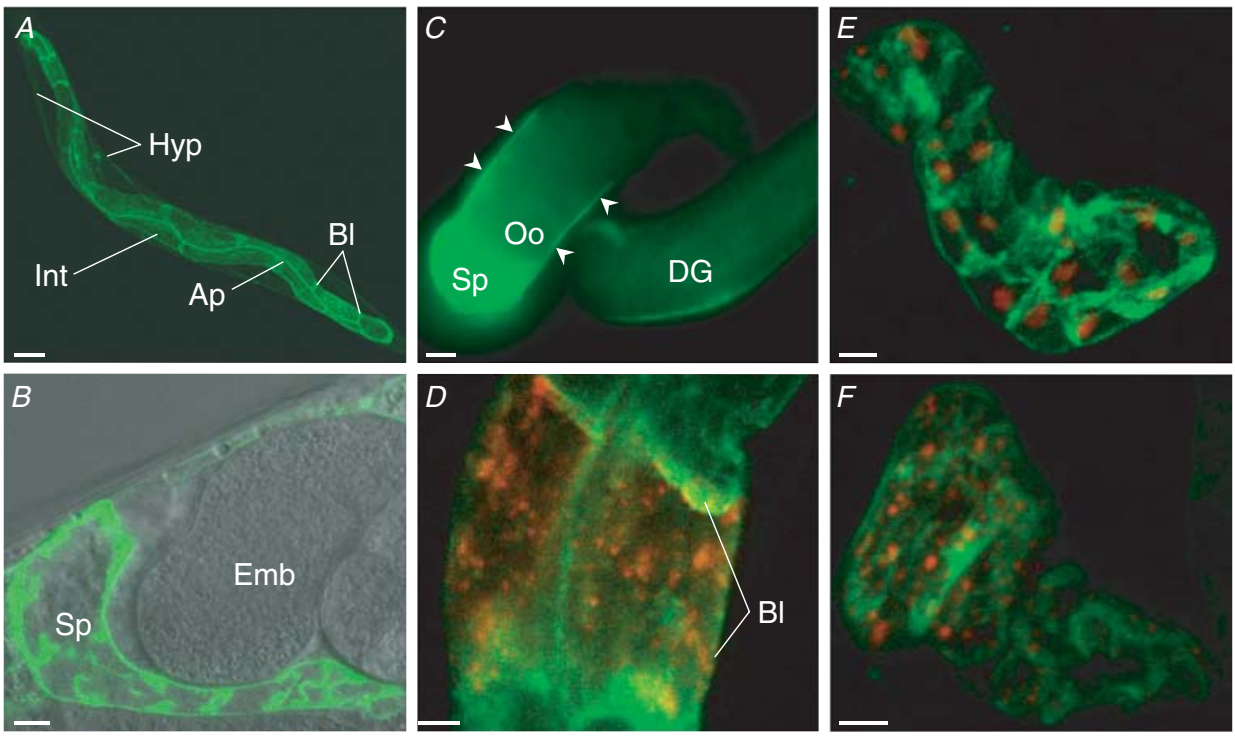

Figure 2. ORAI-1 expression pattern
A, low-magnification confocal 3D reconstruction of ORAI-1::GFP expression pattern in an intact worm. Expression was detected throughout the intestine (Int) and appeared to be localized to apical (Ap) and basolateral (Bl) membrane regions. Weaker fluorescence was also detected throughout the hypodermis (Hyp). Scale bar is 50 μm. *B*, combined DIC and fluorescence confocal micrographs showing ORAI-1::GFP expression in the spermatheca (Sp). Scale bar is 5 μm. Emb, embryo. *C,* fluorescence micrograph of an isolated gonad dissected from a worm expressing a transcriptional ORAI-1 GFP reporter. P_{orai-1}*::GFP* expression is detected in the spermatheca (Sp) and gonadal sheath cells (arrowheads). Scale bar is 10 μm. Oo, oocyte; DG, distal gonad. *D*, confocal micrograph showing expression of ORAI-1::GFP and STIM-1::DsRed in two cells of the anterior intestine. Bl, basolateral membrane. Scale bar is 5 μm. *E* and *F*, confocal 3D reconstructions of ORAI-1::GFP and STIM-1::DsRed expression in the spermatheca. Scale bars are 5 μm.

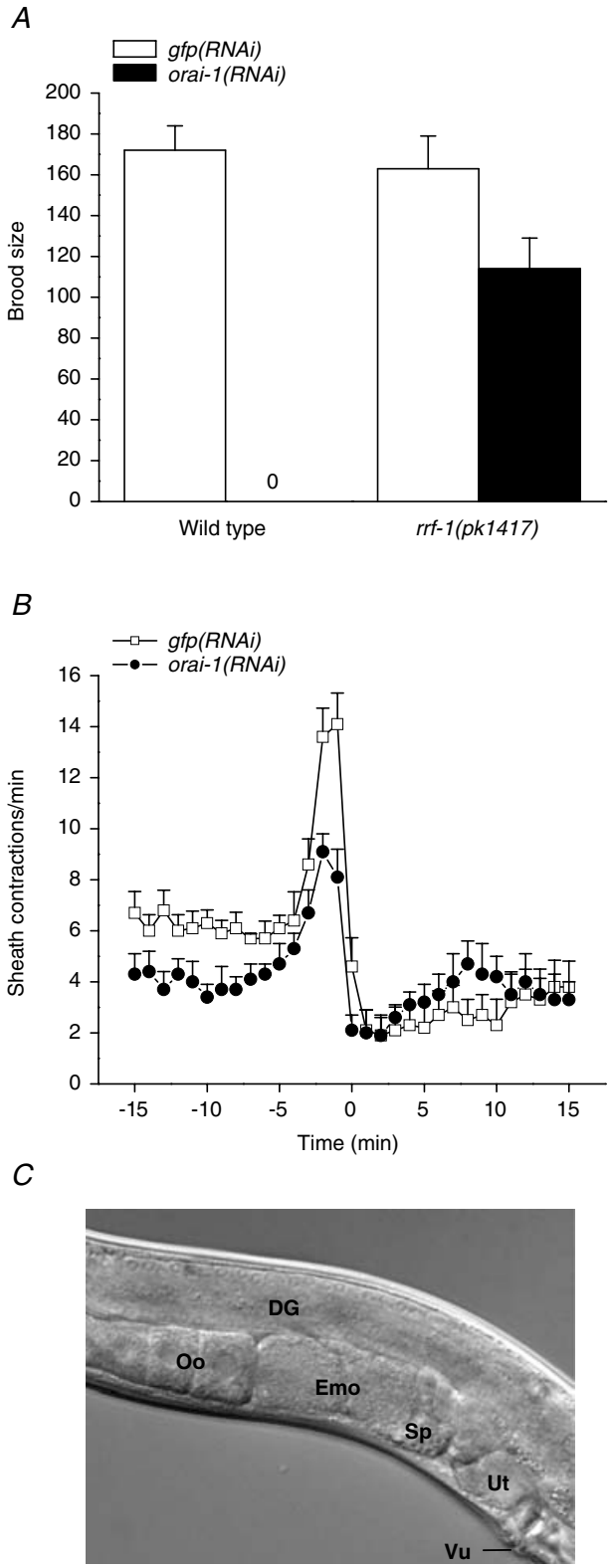

Figure 3. Effect of *orai-1* RNAi on fertility and ovulation
A, brood size in wild-type and *rrf-1(pk1417)* mutant worms. Brood size is defined as the total number of progeny produced over four days. *rrf-1* encodes an RNA-directed RNA polymerase homologue required for RNAi in somatic but not germ cells. *pk1417* is a predicted *rrf-1* null allele (Sijen *et al.* 2001). Worms were fed GFP or *orai-1* dsRNA-producing bacteria for two generations beginning at the L1 larval stage. Values are means ± S.E.M. ($n = 6$–12). *B*, rates of sheath contraction during a single ovulatory cycle. Time 0 is defined as the time at which ovulation was completed in control worms. *orai-1(RNAi)* worms never ovulated (see Results). Therefore in these animals, time 0 is defined the first time point after peak sheath contraction rate was observed. Values are means ± S.E.M. ($n = 6$–7). Worms were fed dsRNA-producing bacteria for two generations. *C*, differential interference contrast micrograph of the gonad of an *orai-1(RNAi)* worm. The distal spermatheca fails to open during ovulation in *orai-1(RNAi)* worms, and oocytes are trapped in the proximal gonad arm where they undergo endomitosis. DG, Distal gonad; Oo, normal oocytes; Emo, endomitotic oocytes; Sp, spermatheca; Ut, uterus; Vu, vulva. Note that the uterus in the *orai-1(RNAi)* worm is empty due to failure of ovulation. worms fed dsRNA-producing bacteria for two generations.

dissected free from a worm strain (kindly provided by Dr David Baillie) expressing an *orai-1* transcriptional GFP reporter. As shown in Fig. 2*C*, *orai-1* is also expressed in both proximal and distal gonadal sheath cells.

In mammalian and *Drosophila* cells, STIM1 homologues function as ER Ca^{2+} sensors and trigger SOCE and CRAC activation in response to Ca^{2+} store depletion (Liou *et al.* 2005; Zhang *et al.* 2005; Soboloff *et al.* 2006*a*; Spassova *et al.* 2006). Our previous studies on *C. elegans* STIM-1 suggested that STIM-1::GFP is localized to an intracellular compartment in the intestine, spermatheca and gonadal sheath cells (Yan *et al.* 2006). To examine the spatial relationship between ORAI-1 and STIM-1, we generated full length STIM-1 fused at the C-terminus to DsRed, and co-expressed it in worms with ORAI-1::GFP. Strong expression of STIM-1::DsRed was detected primarily in the spermatheca and anterior and posterior intestine. Figure 2*D* shows STIM-1::DsRed and ORAI-1::GFP expression in two cells in the anterior intestine. STIM-1 is localized to intracellular puncta, whereas ORAI-1 is primarily localized to a plasma membrane region.

Two patterns of STIM-1::DsRed expression were observed in the spermatheca. In some worms, STIM-1::DsRed localized to large puncta, with individual spermatheca cells appearing to contain only a single site of STIM-1::DsRed expression (Fig. 2*E*). The spermatheca cells of other worms, in contrast, contained numerous smaller STIM-1::DsRed puncta (Fig. 2*F*).

ORAI–1 is required for Ca^{2+}- and IP_3-dependent contractile activity of sheath cells and the spermatheca

Knockdown of *orai-1* expression by RNAi beginning at the L1 larval stage significantly ($P < 0.0001$) reduced mean ± S.E.M.. brood size from 145 ± 8 ($n = 9$) in control worms fed GFP dsRNA-producing bacteria to 18 ± 8 ($n = 12$) in worms fed *orai-1* dsRNA. Continued feeding of *orai-1* dsRNA-producing bacteria to the offspring of these worms caused complete sterility (Fig. 3*A*). Other

than the fertility defect, young adult *orai-1(RNAi)* worms appeared healthy and exhibited no obvious defects in external morphology, movement or feeding behaviour.

Somatic cells of *rrf-1(pk1417)* mutant worms are resistant to dsRNA, but their germline shows a normal RNAi response (Sijen *et al.* 2001). The sterility observed in worms fed *orai-1* dsRNA-producing bacteria was rescued by the *rrf-1(pk1417)* mutation. Worms fed *orai-1* dsRNA-producing bacteria beginning at the L1 larval stage had a mean ± S.E.M. brood size of 138 ± 13 ($n = 11$) that was not significantly ($P > 0.4$) different from that of *gfp(RNAi)* worms (mean ± S.E.M. brood size = 157 ± 16; $n = 6$). Brood size in the F1 offspring of *orai-1(RNAi); rrf-1(pk1417)* worms was slightly but significantly ($P < 0.05$) reduced compared to control animals (Fig. 3*A*). The rescue of fertility in *orai-1(RNAi)* worms by the *rrf-1(pk1417)* mutation indicates that *orai-1* RNAi-induced sterility is due largely to dysfunction of somatic cells.

Adult *C. elegans* hermaphrodites possess two U-shaped gonad arms connected via spermatheca to a common uterus. Oocytes form in the proximal gonad arm and accumulate in a single-file row of graded developmental stages. Developing oocytes remain in diakinesis of prophase I until they reach the most proximal position in the gonad arm, where they undergo meiotic maturation and are then ovulated into the spermatheca for fertilization (reviewed by Hubbard & Greenstein, 2000).

Oocytes are surrounded by myoepithelial sheath cells (Hall *et al.* 1999). Prior to ovulation, sheath cells contract weakly and slowly (McCarter *et al.* 1999). Release of the EGF-like protein LIN-3 from the maturing oocyte induces ovulation by increasing the rate and force of sheath cell contractions and by triggering opening of the distal spermatheca (Iwasaki *et al.* 1996; McCarter *et al.* 1999; Yin *et al.* 2004). The contractile activity of both the sheath cells (Yin *et al.* 2004) and spermatheca (Clandinin *et al.* 1998; Bui & Sternberg, 2002; Kariya *et al.* 2004) is regulated by IP_3 and Ca^{2+} signalling. In addition, we have recently shown that a *C. elegans* homologue of human STIM1 is required for sheath cell and spermatheca function (Yan *et al.* 2006).

Given that *orai-1* RNAi causes sterility by disrupting somatic cell function (Fig. 3*A*), we examined the contractile activity of the sheath cells and spermatheca in dsRNA-fed worms. Figure 3*B* demonstrates that *orai-1* RNAi reduces sheath cell contractions under basal conditions and during ovulation. The mean rates of basal sheath cell contraction measured at –10 min in *gfp(RNAi)* control and *orai-1(RNAi)* worms were 6.3 contractions min^{-1} and 3.4 contractions min^{-1}, respectively. During ovulation, sheath contraction increased significantly ($P < 0.0001$) to a peak rate of 14.2 contractions min^{-1} in control worms and 9.1 contractions min^{-1} in *orai-1(RNAi)* animals. Both basal and peak rates of sheath contraction were significantly ($P < 0.004$) reduced by silencing of *orai-1* expression.

Spermatheca function was also defective in *orai-1(RNAi)* worms. During ovulation, the distal spermatheca opens allowing contracting sheath cells to pull the spermatheca over the maturing oocyte (Hubbard & Greenstein, 2000). In 35 young adult *orai-1(RNAi)* worms examined, the distal spermatheca failed to open during ovulation attempts. Maturing oocytes were therefore trapped in the proximal gonad arm where they underwent endomitosis (Fig. 3*C*). Two worms examined showed what appeared to be incomplete spermatheca opening. Maturing oocytes partially entered the spermatheca but were then pinched off and broken into two pieces, one of which remained trapped in the proximal gonad arm.

ORAI-1 is required for SOCC activity in intestinal epithelial cells but plays no role in IP_3-dependent oscillatory Ca^{2+} signalling

Defecation in *C. elegans* is an ultradian rhythm mediated by sequential contraction of the posterior body wall muscles, anterior body wall muscles and enteric muscles (Iwasaki & Thomas, 1997). Posterior body wall muscle contraction (pBoc) is controlled by IP_3-dependent Ca^{2+} oscillations in intestinal epithelial cells (Dal Santo *et al.* 1999; Espelt *et al.* 2005; Teramoto & Iwasaki, 2006). Oscillatory Ca^{2+} signalling is thought to be critically dependent on SOCE (Parekh & Penner, 1997; Venkatachalam *et al.* 2002; Parekh & Putney, 2005). However, we have shown previously that oscillatory Ca^{2+} signalling in the intestine is unaffected by silencing of *C. elegans stim-1* (Yan *et al.* 2006).

To further examine the role of SOCE in intestinal Ca^{2+}-signalling events, we quantified pBoc in wild-type worms fed *orai-1* dsRNA-producing bacteria for two generations. The effectiveness of *orai-1* RNAi was first assessed by quantifying whole-worm ORAI-1::GFP fluorescence. As shown in Fig. 4*A*, *orai-1* RNAi dramatically and significantly ($P < 0.001$) reduced ORAI-1::GFP expression. Whole-worm fluorescence in ORAI-1::GFP worms was increased 2.85-fold relative to wild-type animals. When these worms were fed *orai-1* dsRNA-producing bacteria for one generation, total fluorescence was reduced to ∼90% of wild-type worm background autofluorescence levels. However, despite this strong knockdown, pBoc period and rhythmicity in *orai-1(RNAi)* worms were not significantly ($P > 0.3$) different from control animals fed GFP dsRNA-producing bacteria (Fig. 4*B*).

We also directly assessed the effect of *orai-1* RNAi on Ca^{2+} oscillations in isolated intestines (Espelt *et al.* 2005). To maximize ORAI-1 knockdown, intestines were

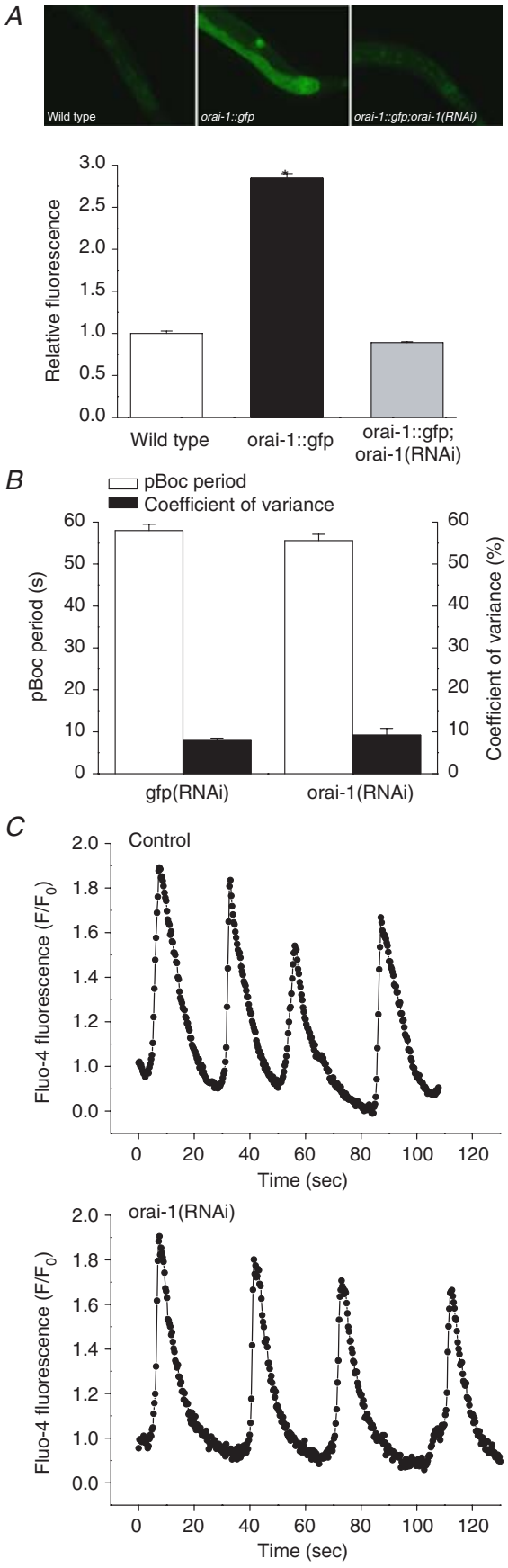

dissected from *rde-1(ne219);kbEx200* worms fed *orai-1* dsRNA-producing bacteria for 2–5 generations. *rde-1* (*R*NAi *de*fective) encodes a protein involved in translation initiation (Tabara *et al.* 1999; Fagard *et al.* 2000) and *rde-1* loss-of-function mutants are strongly resistant to RNAi induced by dsRNA injection, feeding or expression (Tabara *et al.* 1999). *Rde-1* is rescued selectively in the intestines of *rde-1(ne219);kbEx200* worms (Espelt *et al.* 2005), thus allowing us to knockdown intestinal gene expression while maintaining normal fertility. As shown in Fig. 4*C* and Table 1, Ca^{2+} oscillation periods and oscillation rise and fall times were not significantly ($P > 0.06$) different in control and *orai-1(RNAi)* worms.

In *Drosophila* and mammalian cells, the *Orai* and *Orai1* genes are thought to encode store-operated CRAC channels (Prakriya *et al.* 2006; Vig *et al.* 2006*a*; Yeromin *et al.* 2006). Cultured intestinal cells express a SOCC current with many of the same biophysical characteristics as I_{CRAC} (Estevez *et al.* 2003). We therefore examined the effect of *orai-1* RNAi on SOCC activity using whole-cell patch clamp. To maximize *orai-1* knockdown, we cultured intestinal cells from *rde-1(ne219);kbEx200* worms fed *orai-1* dsRNA-producing bacteria for three generations, and included *orai-1* dsRNA in the culture medium at the time of cell plating. Figure 5*A* shows current–voltage relationships of whole-cell currents measured after 5 min of intracellular Ca^{2+} store depletion in a control cell and a cell exposed to *orai-1* dsRNA. Inwardly rectifying store-operated Ca^{2+} current is detected in the control intestinal cell but not in the *orai-1* dsRNA-treated intestinal cell. Mean whole-cell SOCC current density measured at −120 mV in control cells was −25.6 pA pF^{-1}. *orai-1*

Figure 4. Effect of *orai-1* RNAi on ORAI-1 expression, pBoc and intestinal Ca^{2+} signalling
A, effect of *orai-1* RNAi on ORAI-1::GFP expression. Top: fluorescence micrographs of wild-type and ORAI-1::GFP-expressing worms fed bacteria containing the empty RNAi feeding empty RNAi feeding vector and ORAI-1::GFP expressing worms fed *orai-1* dsRNA producing bacteria [*orai-1*:: gfp; *orai-1* (RNAi)]. Fluorescence in wild-type worms is background autofluorescence. Bottom: relative whole-animal fluorescence in wild-type, *orai-1:gfp* and *orai-1::gfp; orai-1(RNAi)* worms. Wild-type and *orai-1:gfp* worms were fed bacteria containing the empty feeding vector. Values are mean ± S.E.M. ($n = 164$–532). $^*P < 0.001$ compared to wild-type and *orai-1::gfp* animals. Whole-worm fluorescence was quantified using a COPAS Biosort and normalized to time-of-flight (i.e. fluorescence/time-of-flight), which is a measure of worm size. RNAi feeding was carried out for one generation. GFP-expressing worms were the integrated strain *KbIs18 (Porai-1::ORAI-1::GFP; Pstim-1::STIM-1::DsRed; rol-6(su1006))*. *B*, effect of *orai-1* RNAi on pBoc period and coefficient of variance, which is a measure of cycle rhythmicity. Wild-type worms were fed GFP or *orai-1* dsRNA-producing bacteria for two generations. Values are means ± S.E.M. ($n = 9$–15). *C*, examples of Ca^{2+} oscillations observed in intestines isolated from *rde-1(ne219);kbEx200* worms fed bacteria containing the empty feeding vector (control) or *orai-1* dsRNA-producing bacteria for two generations. Fluorescent images were acquired at 3 Hz.

Table 1. Effect of *orai-1* RNAi on intestinal Ca^{2+} oscillations

Experiment	Oscillation period (s)	Oscillation rise time (s)	Oscillation fall time (s)
Empty vector	33 ± 2 (14)	5 ± 0.3 (22)	17 ± 1 (20)
Orai-1 RNAi	27 ± 2 (15)	5 ± 0.3 (34)	15 ± 1 (33)

Calcium oscillations were measured in *rde-1(ne219); kbEx200* worms fed *orai-1* dsRNA-producing bacteria or bacteria containing the empty feeding vector for 2–5 generations. Values are means ± S.E.M. Number of observations (*n*) is shown in parentheses.

RNAi significantly ($P < 0.003$) reduced whole-cell SOCC current density to –1.6 pA pF^{-1} (Fig. 5*B*). The inhibitory effect of *orai-1* RNAi is comparable to that of *stim-1* RNAi reported by us previously (Yan *et al.* 2006). Taken together, data in Figs 4 and 5 and Table 1 suggest that SOCC activity is not required for generation of Ca^{2+} oscillations in intestinal epithelial cells. An alternative interpretation is that the small amounts of channel activity that remain after RNAi treatment are sufficient to maintain ER Ca^{2+} store levels and normal cytoplasmic Ca^{2+} signals.

ORAI-1 and STIM-1 interact functionally and mediate SOCC activity

Mutation of the EF hand domain of *Drosophila* and human STIM homologues constitutively activates SOCE and I_{CRAC} (Zhang *et al.* 2005; Liou *et al.* 2005; Soboloff *et al.* 2006*a*; Spassova *et al.* 2006). Transgenic worms expressing a *C. elegans stim-1* EF hand mutant tagged with GFP (i.e. STIM-1(D55A; D57A::GFP)) are sterile and exhibit an increased pBoc period and pBoc arrhythmia (Yan *et al.* 2006). To determine whether ORAI-1 functions together with STIM-1, we fed *stim-1(D55A; D57A)::gfp* worms *orai-1* dsRNA-producing bacteria. As shown in Fig. 6, the increased pBoc period induced by STIM-1(D55A; D57A)::GFP expression was suppressed completely ($P < 0.01$) by *orai-1* RNAi, indicating that *orai-1* and *stim-1* function together in a common pathway. Unlike our previous studies (Yan *et al.* 2006), we found that pBoc rhythmicity, as measured by the coefficient of variance, was not significantly ($P > 0.05$) different in control and *stim-1(D55A;D57A)::gfp* worms. Knockdown of *orai-1* expression in *stim-1(D55A;D57A)::gfp* animals had no significant ($P > 0.05$) effect on CV.

Co-transfection of cells with human or *Drosophila* STIM and Orai1 homologues dramatically increases SOCE and I_{CRAC} (Mercer *et al.* 2006; Peinelt *et al.* 2006; Prakriya & Lewis, 2006; Soboloff *et al.* 2006*b*; Vig *et al.* 2006*a*; Yeromin *et al.* 2006). To further examine the relationship between *C. elegans* ORAI-1 and STIM-1 then, we co-expressed the proteins in HEK293 cells

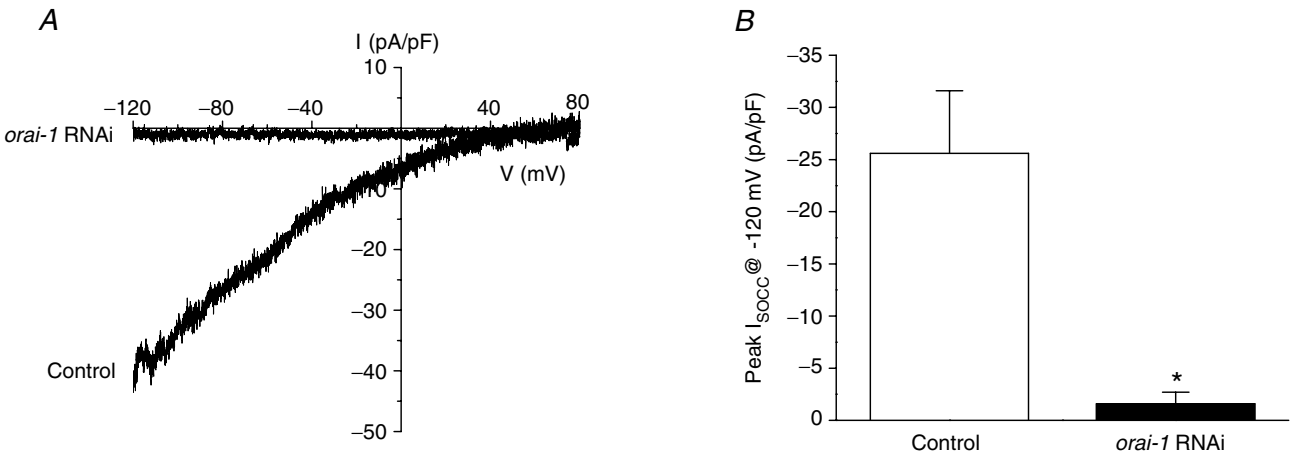

Figure 5. Effect of *orai-1* RNAi on SOCC activity in cultured intestinal cells
A, examples of whole-cell current–voltage relationships of SOCC currents induced by 5 min of store depletion in a control cell and a cell treated with *orai-1* dsRNA. Store depletion was induced using a pipette solution containing 10 μM IP_3, 10 mM BAPTA and 18 nM free-Ca^{2+}. Currents were elicited by ramping membrane voltage from –120 mV to +80 mV at 200 mV s^{-1} every 5 s. *B*, effect of *orai-1* dsRNA on peak I_{SOCC} measured 5 min after obtaining whole-cell access. Values are means ± S.E.M. ($n = 7$–10). *$P < 0.003$ compared to control. Intestinal cells were cultured from *rde-1(ne219);kbEx200* worms (Espelt *et al.* 2005) fed *orai-1* dsRNA-producing bacteria for three generations. *orai-1* dsRNA was also included in the culture medium beginning at the time of cell plating. Cells were patch clamped 2–3 days after isolation from worm embryos.

and performed whole-cell patch-clamp measurements. Intracellular Ca^{2+} stores were depleted by dialysing cells with a solution containing 10 μM IP_3, 10 mM BAPTA and a free Ca^{2+} concentration of ~18 nM. SOCC currents were undetectable in HEK293 cells expressing GFP alone, and in cells co-expressing STIM-1 and GFP or ORAI-1 and GFP (Fig. 7*A*). However, co-expression of STIM-1 and ORAI-1 dramatically increased whole-cell current (Fig. 7*A* and *B*). The current showed strong inward rectification (Fig. 7*B*) and was not gated by membrane voltage (Fig. 7*C*). Current density was quite variable from cell-to-cell, and ranged between –11 pA pF^{-1} and –66 pA pF^{-1}. Mean current density at –120 mV observed 5 min after whole-cell access was obtained was –31.0 pA pF^{-1} ($n = 15$). No current was detected in STIM-1/ORAI-1 co-transfected cells in the absence of store depletion (Fig. 7*A* and *B*).

The *C. elegans* intestinal cell SOCC current shares many similarities with mammalian I_{CRAC}. However, the current also exhibits some distinct differences. Unlike *Drosophila* and mammalian I_{CRAC}, *C. elegans* I_{SOCC} is not activated by low concentrations of 2-APB, has a relatively high Cs^+ permeability and shows much slower rundown or 'depotentiation' when exposed to divalent cation-free (DVF) extracellular solution (Estevez *et al.* 2003; Yeromin *et al.* 2004). To determine whether heterologous expression of STIM-1 and ORAI-1 recapitulates the properties of the endogenous intestinal I_{SOCC}, we characterized 2-APB sensitivity, Cs^+ permeability and depotentiation. As shown in Figs 8*A* and *B*, 5 μM 2-APB had no significant ($P > 0.9$) effect on current amplitude, while exposure to 100 μM 2-APB inhibited the current ~60% ($P < 0.0002$).

The effect of DVF bath on whole-cell current was complex. Out of 30 successful recordings, we observed only two cells that exhibited the typical response to DVF bath where current amplitude increased rapidly and then underwent slow depotentiation upon removal of extracellular divalent cations (Fig. 9*A*). Rates of current depotentiation in the two cells were –11% min^{-1} and –19% min^{-1}. These values are comparable to the mean rate of depotentiation of –13% min^{-1} seen in cultured *C. elegans* intestinal cells (Estevez *et al.* 2003). Both cells had measurable outward currents and reversal potentials of 8.8 mV and 14.6 mV in the DVF bath. In one cell, Na^+ in the bath solution was successfully replaced with Cs^+, which shifted E_{rev} by –9.1 mV. The calculated Cs^+ permeability relative to Na^+ (i.e. P_{Cs}/P_{Na}) was 0.7, which is similar to the mean intestinal SOCC P_{Cs}/P_{Na} of 0.6 (Estevez *et al.* 2003).

The two cells that exhibited the typical response to DVF bath had current densities of 5.9 pA pF^{-1} and 7.3 pA pF^{-1}. We refer to these cells as 'low-current' cells. All other cells in which these DVF experiments were performed successfully had current densities of 30–60 pA pF^{-1}, and we refer to these as 'high-current' cells. The response to DVF bath in high-current cells contrasted sharply with that of low-current cells. In 28 out of 28 high-current cells, removal of bath divalent cations rapidly and nearly completely inhibited whole-cell current. Current inhibition was followed by slow current reactivation (Fig. 9*B*). The reactivated current showed both inward and outward components, and reversed at a mean ± S.E.M. value of 12.0 ± 2.4 mV ($n = 5$). Replacement of bath Na^+ with Cs^+ shifted E_{rev} by a mean ± S.E.M. value of –31.6 ± 3.2 mV. The mean ± S.E.M. P_{Cs}/P_{Na} calculated from this shift was 0.3 ± 0.04 ($n = 5$).

The different response to DVF bath of low- and high-current cells suggested that channel expression level and whole-cell current amplitude somehow alter channel regulation. Attempts to increase the proportion of low-current cells were unsuccessful. Reducing transfection time to 3 h, or transfecting cells with 10-fold less (i.e. 0.1 μg) ORAI-1 and STIM-1 cDNA did not increase the frequency of low-current cells, but instead increased the number of cells lacking measurable SOCC currents.

Interestingly, in two high-current cells, we were able to switch back to a 10 mM Ca^{2+} bath after an exposure to DVF medium of several minutes. When these cells were exposed a second time to DVF bath, current amplitude increased rapidly as expected (data not shown). Regulation of CRAC channels by intracellular Ca^{2+} concentration has

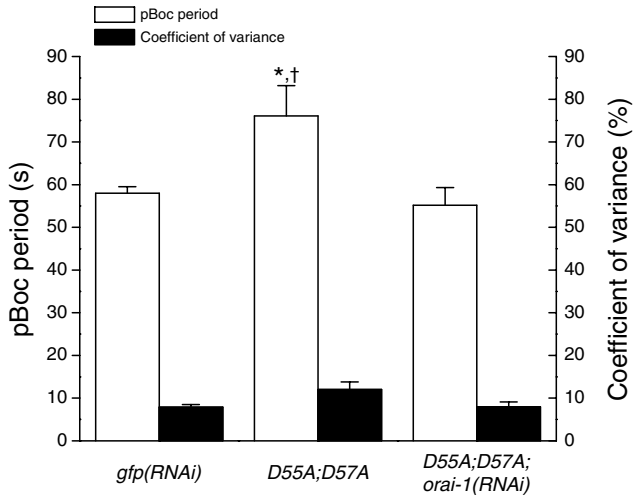

Figure 6. Effect of *orai-1* RNAi on pBoc period and coefficient of variance in transgenic worms expressing the GFP-tagged STIM-1 EF hand mutant protein STIM-1(D55A; D57A)::GFP
Data on wild-type worms fed GFP dsRNA-producing bacteria (*gfp(RNAi)*) are reproduced from Fig. 4*B*. *D55A; D57A* worms were fed bacteria containing the empty RNAi feeding vector or bacteria producing *orai-1* dsRNA. RNAi feeding was carried out over two generations. Values are means ± S.E.M. (n = 13–15). *$P < 0.05$ compared to *gfp(RNAi)* worms. †$P < 0.01$ compared to *D55A;D57A* worms fed *orai-1* dsRNA-producing bacteria. pBoc periods in *gfp(RNAi)* and *D55A; D57A; orai-1(RNAi)* worms were not significantly ($P > 0.05$) different. Coefficients of variance in all three groups of worms were not significantly ($P > 0.05$) different.

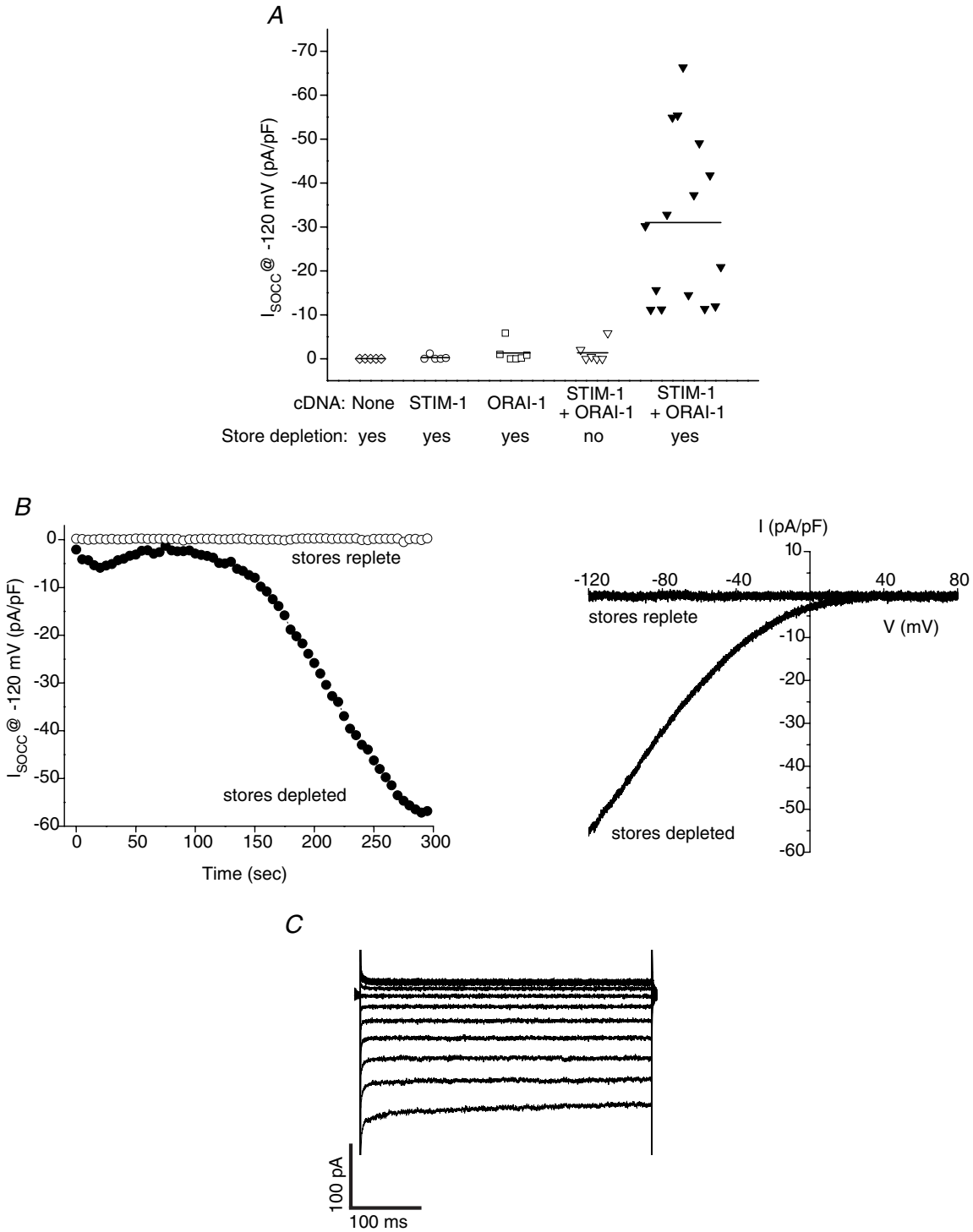

Figure 7. Effect of heterologous expression of ORAI-1 and STIM-1 in HEK293 cells on store-operated currents

A, whole-cell currents in individual HEK293 cells transfected with GFP, STIM-1 and GFP, ORAI-1 and GFP, or STIM-1, ORAI-1 and GFP cDNAs. Solid lines are the mean currents for each of the groups shown. Currents were elicited by ramping membrane voltage from –120 mV to +80 mV at 200 mV s^{-1} every 5 s. Holding potential was 0 mV. The currents shown were those observed 5 min after obtaining whole-cell access and are leak current subtracted. Mean whole-cell current in STIM-1/ORAI-1-expressing cells with depleted stores was significantly ($P < 0.001$) different from the other four groups shown. Store depletion was induced by dialysing cells with a pipette solution containing 10 mM BAPTA, 10 μM IP_3 and ~18 nM free-Ca^{2+}. Depletion of stores was prevented using a pipette solution containing 10 mM BAPTA, 2 mM ATP and ~140 nM free-Ca^{2+}. *B*, examples of time-dependent changes in current

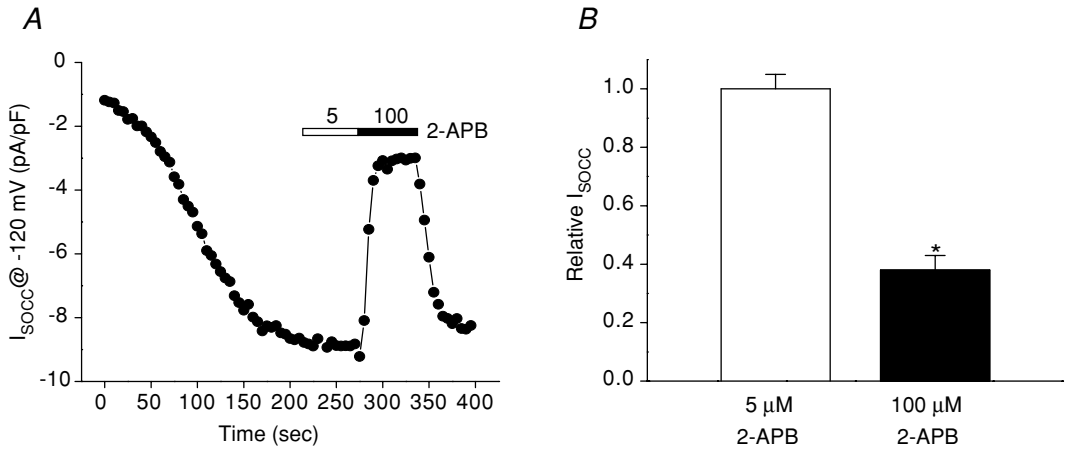

Figure 8. Effect of 2-APB on ORAI-1/STIM-1-induced store-operated currents in HEK293 cells
A, example of the effect of 5 μM (open bar) and 100 μM (filled bar) 2-APB on store-operated current in an ORAI-1/STIM-1-expressing cell. *B*, effect of 5 μM and 100 μM 2-APB on relative whole-cell current in HEK293 cells co-expressing ORAI-1 and STIM-1. Values are means ± S.E.M. ($n = 4$–5). *$P < 0.0002$ compared to control without 2-APB.

been well described (e.g. Zweifach & Lewis, 1995*a*, 1995*b*). Our observation thus suggested the possibility that the anomalous response of high-current cells to extracellular divalent cation removal may be due to high rates of Ca^{2+} influx and intracellular Ca^{2+}-dependent channel regulatory mechanisms. To test this possibility, cells were bathed in an extracellular solution containing 0.25 mM Ca^{2+} before being exposed to DVF medium. We refer to these cells as 'low-Ca^{2+}' cells. In 10 out of 10 low-Ca^{2+} cells, exposure to DVF bath caused an immediate increase in whole-cell current (Fig. 9*C*). This current typically continued to activate slowly and then stabilized (e.g. Fig. 9*C*). Rapid rundown or 'depotentiation' of the current was never observed.

The mean ± S.E.M. E_{rev} in the DVF bath was 22.6 ± 4.0 mV ($n = 5$). Replacement of bath Na^+ with Cs^+ shifted E_{rev} to more negative values. The mean ± S.E.M. Cs^+-induced shift in E_{rev} and calculated P_{Cs}/P_{Na} were –50.0 ± 6.8 mV and 0.2 ± 0.05 ($n = 5$), respectively. The shift in E_{rev} was significantly ($P < 0.04$) different from that observed in high-current cells bathed with 10 mM Ca^{2+}. However, even though there was a difference in the mean P_{Cs}/P_{Na} between the two groups of cells, this difference did not achieve statistical significance ($P > 0.08$). Interestingly, both high-current cells bathed with 10 mM Ca^{2+} and low-Ca^{2+} cells had relative Cs^+ permeabilities that were considerably lower than that of the single low-current cell in which we were able to measure this parameter. Taken together, the effects of low bath Ca^{2+} concentration suggest that normal channel regulation may be altered by high levels of channel expression and concomitant Ca^{2+} influx. This in turn affects the response of the channel, via unknown mechanisms, to removal of extracellular divalent cations. High levels of channel expression may also alter the permeability properties of the channel.

Discussion

The current paper extends our previous findings demonstrating that *C. elegans* possesses a STIM-1 homologue required for SOCC activity and some IP_3-dependent Ca^{2+} signalling processes (Yan *et al.* 2006). As we demonstrate here, a single Orai homologue is also present in the worm genome. *orai-1* and *stim-1* are co-expressed in various cell types (Fig. 2) and RNAi silencing of either gene gives rise to identical phenotypes, namely, loss of intestinal cell SOCC function (Fig. 5) as well as sterility due primarily to disruption of IP_3-dependent spermatheca contractility (Fig. 3 and Results) (Yan *et al.* 2006). ORAI-1 knockdown suppresses the pBoc defect induced by expression of a STIM-1 EF hand Ca^{2+}-binding mutant in the worm intestine (Fig. 6 and Yan *et al.* 2006), indicating that the proteins function

activity (left panel) and current–voltage relationships (right panel) of currents observed in an ORAI-1/STIM-1–expressing cell with replete stores and in an ORAI-1/STIM-1-expressing cell in which stores were depleted. Current–voltage relationships were plotted for currents measured 5 min after obtaining whole-cell access. Leak current was subtracted from the current induced by store depletion. *C*, example of store-operated whole-cell currents elicited by stepping membrane voltage in 20 mV steps from –120 mV to +80 mV in an ORAI-1/STIM-1-expressing cell. Holding potential was 0 mV.

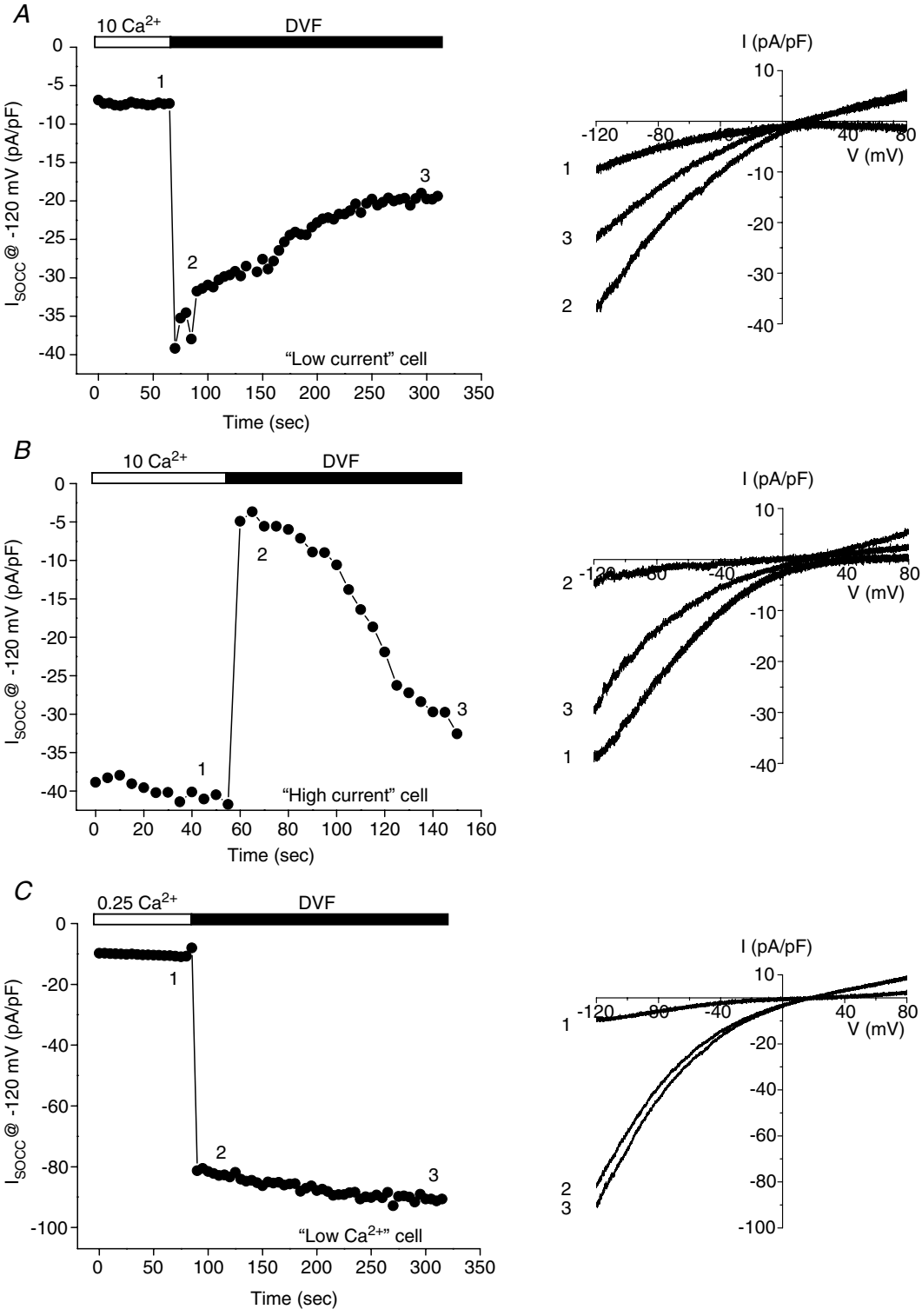

Figure 9. Examples of the effects of divalent cation-free (DVF) bath on store-operated whole-cell currents in different ORAI-1/STIM-1-expressing cells

'Low-current' (*A*) and 'high-current' (*B*) cells had current densities of 6–7 pA pF^{-1} and 30–60 pA pF^{-1}, respectively. The control bath solution for low- and high-current cells contained 10 mM Ca^{2+}. 'Low-Ca^{2+}' (*C*) cells were bathed in an extracellular solution containing 0.25 mM Ca^{2+} before exposure to the DVF bath. Data shown are for single cells. Current–voltage relationships for currents observed in each of the three groups of cells are shown in the right panels. Numbering of the traces corresponds to the times at which the current–voltage relationships were obtained (i.e. left panel).

in a common signalling pathway. In addition, heterologous co-expression of ORAI-1 and STIM-1 gives rise to robust SOCC activity (Fig. 7).

The properties of the native *C. elegans* intestinal SOCC that distinguish it from *Drosophila* and mammalian CRAC channels are lack of stimulation by low concentrations of 2-APB, slow depotentiation in a DVF bath and relatively high Cs^+ permeability (reviewed by Yeromin *et al.* 2004). The ORAI-1/STIM-1-induced SOCC is unaffected by 5 μM 2-APB (Fig. 8) and has a P_{Cs}/P_{Na} 2–7-fold higher than that reported for other CRAC channels. In addition, whole-cell currents that showed a normal response to DVF bathing underwent depotentiation at a rate remarkably similar to that of native SOCC (Fig. 9*A*). We conclude from these results and studies on *Drosophila* and human Orai homologues (Prakriya *et al.* 2006; Vig *et al.* 2006*a*; Yeromin *et al.* 2006), that *C. elegans* possesses a bona fide CRAC channel encoded by *orai-1* and regulated by STIM-1.

The rapid inhibitory effect of bath divalent cation removal observed in cells with high levels of channel activity (Fig. 9*B*) is intriguing. Reducing bath Ca^{2+} concentration from 10 mM to 0.25 mM prevented this inhibitory effect (Fig. 9*C*). This observation suggests that high rates of Ca^{2+} influx alter CRAC channel function and regulation. The underlying mechanism by which this occurs is unclear at present. However, further study of this phenomenon may shed light on the mechanisms by which both extracellular and intracellular Ca^{2+} regulate CRAC channel activity. Our findings also raise a cautionary note. We are unaware of studies showing that native CRAC channels undergo rapid inhibition in response to DVF extracellular solutions. Thus, it is likely that heterologous overexpression alters channel structure/function relationships and/or regulation. Conclusions drawn from heterologous expression studies on CRAC channel function, and in particular regulation, should be tempered by these concerns.

ORAI-1 shares 34–38% amino acid sequence identity with *Drosophila* and human Orai homologues. Not surprisingly, predicted transmembrane domains show considerable sequence homology across widely divergent species that are separated by many hundreds of millions of years of evolution. In addition, there is strong sequence conservation in the intracellular loop located between TM2 and TM3 (Fig. 1). This domain may function critically in channel regulation, perhaps as a site for proposed functional interactions with STIM proteins (Vig *et al.* 2006*a*; Yeromin *et al.* 2006). Conserved proline residues located in the intracellular N-terminus (Fig. 1) probably also play important functional roles.

We conducted BLAST searches using all available genome sequences, and identified STIM-1 and ORAI-1 homologues only in animals. Estimates of the evolutionary origin of nematodes range from 600 to 1300 million years ago (reviewed by Coghlan, 2005). CRAC channels are thus a very ancient animal innovation. Despite their presence in organisms as diverse as roundworms, fruit flies and humans, and their widespread expression in functionally diverse mammalian cell types (Parekh & Penner, 1997; Venkatachalam *et al.* 2002; Parekh & Putney, 2005), the physiological roles of CRAC channels are largely unknown. It is widely stated in the literature that CRAC channels and SOCE are essential for generation of IP_3-dependent Ca^{2+} signals, and for maintenance of ER Ca^{2+} levels during Ca^{2+} signalling events (Parekh & Penner, 1997; Venkatachalam *et al.* 2002; Parekh & Putney, 2005). However, in most cell types, direct evidence supporting this notion is lacking. Furthermore, our previous studies on STIM-1 (Yan *et al.* 2006) and the data presented in this paper suggest that CRAC channel activity is not required for maintenance of ER Ca^{2+} homeostasis or for oscillatory Ca^{2+} signalling in the *C. elegans* intestine (Fig. 4 and Table 1) (Yan *et al.* 2006).

If CRAC channels are not essential components of all Ca^{2+}-signalling pathways, why are they so widely observed and why have the channel's functional/structural properties been conserved from worms to humans? We have suggested previously that a primary function of SOCE may be to provide cells with a failsafe mechanism for protecting store Ca^{2+} levels during pathophysiological insults and exposure to cellular stressors. Bacterial toxins (Bryant *et al.* 2003; Saha *et al.* 2005), viral proteins (Tian *et al.* 1995; van Kuppeveld *et al.* 1997) ischaemia (Lehotsky *et al.* 2003) and oxidants (Henschke & Elliott, 1995; Pariente *et al.* 2001) induce store Ca^{2+} loss and depletion. Failure to maintain store Ca^{2+} levels under pathophysiological and stress conditions can exacerbate injury by disrupting ER protein synthesis and processing, and lead ultimately to cell death (Rao *et al.* 2004; Schroder & Kaufman, 2005).

CRAC channels clearly play critical signalling roles in some cell types. An important role for CRAC channels in immune cell signalling is well established (reviewed by Lewis, 2001), and they are essential for gonad function and fertility in *C. elegans* (Fig. 3 and Yan *et al.* 2006). The functional properties of CRAC channels are probably specialized for certain signalling mechanisms. CRAC channels have a very high Ca^{2+} selectivity and thus will have little effect on membrane potential when they are active and mediating Ca^{2+} influx. While CRAC channels are not gated directly by voltage, membrane potential will alter Ca^{2+} flux by changing the electrical driving force for Ca^{2+}. In addition, CRAC channels have been reported to undergo slow voltage-dependent changes in macroscopic conductance (reviewed by Lewis, 2001; Parekh & Putney, 2005). Thus, variable patterns of CRAC channel-mediated Ca^{2+} influx can be induced by the activity of other plasma membrane ion channels that affect membrane potential. This in turn increases the complexity and information content of Ca^{2+} signals, as well as the rate of store refilling.

Calcium influx through CRAC channels appears to occur at discrete membrane locations where STIM1 proteins accumulate in response to store depletion (Luik *et al.* 2006). Such compartmentalization of Ca^{2+} entry would provide a mechanism for specifically regulating downstream cellular and ER signalling molecules that colocalize with STIM1 proteins and CRAC channels. Regulation of CRAC channel activity by store Ca^{2+} depletion also provides a way to coordinate compartmentalized Ca^{2+} influx with Ca^{2+} efflux through IP_3 receptors and signalling pathways that control levels of IP_3 and associated lipid second messengers.

Our findings suggesting that CRAC is not an essential component of *C. elegans* intestinal Ca^{2+} signalling imply that depletion of ER Ca^{2+} stores does not necessarily occur pari passu with generation of IP_3-dependent Ca^{2+} signals. In most cell types, SOCE and CRAC channel activation has been observed only under conditions of extreme store depletion experimentally induced by SERCA inhibition, supraphysiological IP_3 receptor activation, exposure to high concentrations of ionomycin and/or increases in cytoplasmic Ca^{2+} buffering (e.g. Parekh *et al.* 1997; Golovina *et al.* 2001; Machaca, 2003). Direct measurements of store Ca^{2+} levels during physiologically relevant Ca^{2+} signalling events are lacking. In the one detailed study conducted to date, little or no change in store Ca^{2+} levels was detected during acetylcholine-induced Ca^{2+} oscillations in pancreatic acinar cells. Only during stimulation with supraphysiological acetylcholine concentrations was store depletion observed (Park *et al.* 2000).

It has been suggested that global ER Ca^{2+} levels are unaffected during normal Ca^{2+} signalling events, and that instead Ca^{2+} depletion probably occurs in ER microdomains or cisternae located close to the plasma membrane (e.g. Berridge, 2002, 2004; Penner & Fleig, 2004). However, photobleaching and Ca^{2+}-uncaging experiments suggest that in acinar cells at least, the ER is a continuous compartment and that Ca^{2+} loss from microdomains is rapidly replenished by Ca^{2+} in the bulk ER (Park *et al.* 2000).

The emerging model of CRAC channel regulation by STIM1 homologues also argues against localization of Ca^{2+} depletion to ER microdomains close to the plasma membrane. In Ca^{2+}-replete stores, STIM1 proteins show a diffuse localization in the ER and redistribute to puncta during store depletion (Liou *et al.* 2005; Zhang *et al.* 2005; Wu *et al.* 2006). Elegant studies by Wu *et al.* (2006) have demonstrated that these puncta correspond to ER–plasma membrane contact sites. It is widely accepted that STIM1 homologues function as ER Ca^{2+} sensors (Liou *et al.* 2005; Zhang *et al.* 2005; Soboloff *et al.* 2006*a*; Spassova *et al.* 2006). Since the protein localizes to ER microdomains close to the plasma membrane only during CRAC channel activation, the activating signal cannot be Ca^{2+} depletion in these regions. Thus, STIM1 is either sensing global ER Ca^{2+} levels or Ca^{2+} levels in an as yet to be defined ER microdomain.

Clearly, a complete understanding of the physiological roles of CRAC channels requires direct measurements of ER Ca^{2+} store levels in a variety of cell types both under physiologically relevant conditions and during pathophysiological insults. In immune cells and *C. elegans* sheath and spermatheca cells, ER Ca^{2+} stores presumably become depleted during normal Ca^{2+}-signalling events. Direct measurement of the dynamics of store depletion and refilling in these cell types would be valuable. Do Ca^{2+} stores in immune cells and worm sheath and spermatheca cells become depleted because they have a limited volume and/or because rates of ER Ca^{2+} uptake are slow relative to total store capacity combined with rates of passive Ca^{2+} leak and efflux through activated IP_3 receptors? It is likely that the functional properties of the ER Ca^{2+} stores are specifically tailored to the signalling requirements of the cell and the role of CRAC channels in those signalling pathways.

In summary, we have identified a *C. elegans* Orai1 homologue that encodes a CRAC channel regulated by STIM-1. The *C. elegans* CRAC channel is the evolutionarily oldest example of this highly specialized channel type that has been described to date. Our current studies along with our previous work on *C. elegans* STIM-1 (Yan *et al.* 2006) argue that CRAC channels and SOCE are not obligate components of all IP_3-dependent Ca^{2+}-signalling pathways. Instead, we suggest that CRAC channels carry out specialized signalling functions that are tailored to the physiological requirements of the cell, and that they also may function to protect cells from pathophysiological insults and stressors that disrupt ER Ca^{2+} homeostasis. The identification of Orai1 and STIM1 proteins has now made it possible to precisely define the physiological roles and regulation of CRAC channels and to determine whether they will be useful targets for treatment of human disease.

References

Baba Y, Hayashi K, Fujii Y, Mizushima A, Watarai H, Wakamori M, Numaga T, Mori Y, Iino M, Hikida M & Kurosaki T (2006). Coupling of STIM1 to store-operated Ca^{2+} entry through its constitutive and inducible movement in the endoplasmic reticulum. *Proc Natl Acad Sci U S A* **103**, 16704–16709.

Berridge MJ (2002). The endoplasmic reticulum: a multifunctional signaling organelle. *Cell Calcium* **32**, 235–249.

Berridge M (2004). Conformational coupling: a physiological calcium entry mechanism. *Sci STKE* **2004**, e33.

Berridge MJ, Bootman MD & Roderick HL (2003). Calcium signalling: dynamics, homeostasis and remodelling. *Nat Rev Mol Cell Biol* **4**, 517–529.

Brenner S (1974). The genetics of *Caenorhabditis elegans*. *Genetics* **77**, 71–94.

Bryant AE, Bayer CR, Hayes-Schroer SM & Stevens DL (2003). Activation of platelet gpIIbIIIa by phospholipase C from *Clostridium perfringens* involves store-operated calcium entry. *J Infect Dis* **187**, 408–417.

Bui YK & Sternberg PW (2002). *Caenorhabditis elegans* inositol 5-phosphatase homolog negatively regulates inositol 1,4,5-triphosphate signaling in ovulation. *Mol Biol Cell* **13**, 1641–1651.

Christensen M, Estevez AY, Yin XM, Fox R, Morrison R, McDonnell M, Gleason C, Miller DM & Strange K (2002). A primary culture system for functional analysis of *C. elegans* neurons and muscle cells. *Neuron* **33**, 503–514.

Clandinin TR, DeModena JA & Sternberg PW (1998). Inositol trisphosphate mediates a RAS-independent response to LET-23 receptor tyrosine kinase activation in *C. elegans*. *Cell* **92**, 523–533.

Coghlan A (2005). Nematode genome evolution In *Wormbook*, www.wormbook.org/chapters/www˙genomevol/genomevol.html.

Dal Santo P, Logan MA, Chisholm AD & Jorgensen EM (1999). The inositol trisphosphate receptor regulates a 50-second behavioral rhythm in *C. elegans*. *Cell* **98**, 757–767.

Espelt MV, Estevez AY, Yin X & Strange K (2005). Oscillatory Ca^{2+} signaling in the isolated *Caenorhabditis elegans* intestine: role of the inositol-1,4,5-trisphosphate receptor and phospholipases C β and γ. *J Gen Physiol* **126**, 379–392.

Estevez AY, Roberts RK & Strange K (2003). Identification of store-independent and store-operated Ca^{2+} conductances in *Caenorhabditis elegans* intestinal epithelial cells. *J General Physiol* **122**, 207–223.

Fagard M, Boutet S, Morel JB, Bellini C & Vaucheret H (2000). AGO1, QDE-2, and RDE-1 are related proteins required for post-transcriptional gene silencing in plants, quelling in fungi, and RNA interference in animals. *Proc Natl Acad Sci U S A* **97**, 11650–11654.

Feske S, Gwack Y, Prakriya M, Srikanth S, Puppel SH, Tanasa B, Hogan PG, Lewis RS, Daly M & Rao A (2006). A mutation in Orai1 causes immune deficiency by abrogating CRAC channel function. *Nature* **441**, 179–185.

Fukushige T, Hawkins MG & McGhee JD (1998). The GATA-factor *elt-2* is essential for formation of the *Caenorhabditis elegans* intestine. *Dev Biol* **198**, 286–302.

Golovina VA, Platoshyn O, Bailey CL, Wang J, Limsuwan A, Sweeney M, Rubin LJ & Yuan JX (2001). Upregulated TRP and enhanced capacitative Ca^{2+} entry in human pulmonary artery myocytes during proliferation. *Am J Physiol Heart Circ Physiol* **280**, H746–H755.

Hall DH, Winfrey VP, Blaeuer G, Hoffman LH, Furuta T, Rose KL, Hobert O & Greenstein D (1999). Ultrastructural features of the adult hermaphrodite gonad of *Caenorhabditis elegans*: relations between the germ line and soma. *Dev Biol* **212**, 101–123.

Henschke PN & Elliott SJ (1995). Oxidized glutathione decreases luminal Ca^{2+} content of the endothelial cell ins (1,4,5) P_3-sensitive Ca^{2+} store. *Biochem J* **312**, 485–489.

Hobert O (2002). PCR fusion-based approach to create reporter gene constructs for expression analysis in transgenic *C. elegans*. *Biotechniques* **32**, 728–730.

Hoth M & Penner R (1992). Depletion of intracellular calcium stores activates a calcium current in mast cells. *Nature* **355**, 353–356.

Hubbard EJ & Greenstein D (2000). The *Caenorhabditis elegans* gonad: a test tube for cell and developmental biology. *Dev Dyn* **218**, 2–22.

Iwasaki K, McCarter J, Francis R & Schedl T (1996). *emo-1*, a *Caenorhabditis elegans* Sec61p gamma homologue, is required for oocyte development and ovulation. *J Cell Biol* **134**, 699–714.

Iwasaki K & Thomas JH (1997). Genetics in rhythm. *Trends Genet* **13**, 111–115.

Kamath RS, Martinez-Campos M, Zipperlen P, Fraser AG & Ahringer J (2000). Effectiveness of specific RNA-mediated interference through ingested double-stranded RNA in *Caenorhabditis elegans*. *Genome Biol* **2**, 2.1–2.2.10.

Kariya K, Kim BY, Gao X, Sternberg PW & Kataoka T (2004). Phospholipase Cϵ regulates ovulation in *Caenorhabditis elegans*. *Dev Biol* **274**, 201–210.

Lehotsky J, Kaplan P, Babusikova E, Strapkova A & Murin R (2003). Molecular pathways of endoplasmic reticulum dysfunctions: possible cause of cell death in the nervous system. *Physiol Res* **52**, 269–274.

Lewis RS (2001). Calcium signaling mechanisms in T lymphocytes. *Annu Rev Immunol* **19**, 497–521.

Liou J, Kim ML, Heo WD, Jones JT, Myers JW, Ferrell JE Jr & Meyer T (2005). STIM is a Ca^{2+} sensor essential for Ca^{2+}-store-depletion-triggered Ca^{2+} influx. *Curr Biol* **15**, 1235–1241.

Luik RM, Wu MM, Buchanan J & Lewis RS (2006). The elementary unit of store-operated Ca^{2+} entry: local activation of CRAC channels by STIM1 at ER–plasma membrane junctions. *J Cell Biol* **174**, 815–825.

Machaca K (2003). Ca^{2+}-calmodulin-dependent protein kinase II potentiates store-operated Ca^{2+} current. *J Biol Chem* **278**, 33730–33737.

McCarter J, Bartlett B, Dang T & Schedl T (1999). On the control of oocyte meiotic maturation and ovulation in *Caenorhabditis elegans*. *Dev Biol* **205**, 111–128.

Mello CC, Kramer JM, Stinchcomb D & Ambros V (1991). Efficient gene transfer in *C. elegans*: extrachromosomal maintenance and integration of transforming sequences. *EMBO J* **10**, 3959–3970.

Mercer JC, Dehaven WI, Smyth JT, Wedel B, Boyles RR, Bird GS & Putney JW Jr (2006). Large store-operated calcium-selective currents due to co-expression of Orai1 or Orai2 with the intracellular calcium sensor, Stim1. *J Biol Chem* **281**, 24979–24990.

Parekh AB, Fleig A & Penner R (1997). The store-operated calcium current I_{CRAC}: nonlinear activation by $InsP_3$ and dissociation from calcium release. *Cell* **89**, 973–980.

Parekh AB & Penner R (1997). Store depletion and calcium influx. *Physiol Rev* **77**, 901–930.

Parekh AB & Putney JW (2005). Store-operated calcium channels. *Physiol Rev* **85**, 757–810.

Pariente JA, Camello C, Camello PJ & Salido GM (2001). Release of calcium from mitochondrial and nonmitochondrial intracellular stores in mouse pancreatic acinar cells by hydrogen peroxide. *J Membr Biol* **179**, 27–35.

Park MK, Petersen OH & Tepikin AV (2000). The endoplasmic reticulum as one continuous Ca^{2+} pool: visualization of rapid Ca^{2+} movements and equilibration. *EMBO J* **19**, 5729–5739.

Peinelt C, Vig M, Koomoa DL, Beck A, Nadler MJ, Koblan-Huberson M, Lis A, Fleig A, Penner R & Kinet JP (2006). Amplification of CRAC current by STIM1 and CRACM1 (Orai1). *Nat Cell Biol* **8**, 771–773.

Penner R & Fleig A (2004). Store-operated calcium entry: a tough nut to CRAC. *Sci. STKE* 2004, e38.

Prakash YS, Kannan MS & Sieck GC (1997). Regulation of intracellular calcium oscillations in porcine tracheal smooth muscle cells. *Am J Physiol Cell Physiol* **272**, C966–C975.

Prakriya M, Feske S, Gwack Y, Srikanth S, Rao A & Hogan PG (2006). Orai1 is an essential pore subunit of the CRAC channel. *Nature* **443**, 230–233.

Prakriya M & Lewis RS (2006). Regulation of CRAC channel activity by recruitment of silent channels to a high open-probability gating mode. *J Gen Physiol* **128**, 373–386.

Rao RV, Ellerby HM & Bredesen DE (2004). Coupling endoplasmic reticulum stress to the cell death program. *Cell Death Differ* **11**, 372–380.

Roos J, DiGregorio PJ, Yeromin AV, Ohlsen K, Lioudyno M, Zhang S, Safrina O, Kozak JA, Wagner SL, Cahalan MD, Velicelebi G & Stauderman KA (2005). STIM1, an essential and conserved component of store-operated Ca^{2+} channel function. *J Cell Biol* **169**, 435–445.

Rual JF, Ceron J, Koreth J, Hao T, Nicot AS, Hirozane-Kishikawa T, Vandenhaute J, Orkin SH, van den Hill DE, HS & Vidal M (2004). Toward improving *Caenorhabditis elegans* phenome mapping with an ORFeome-based RNAi library. *Genome Res* **14**, 2162–2168.

Saha S, Gupta DD & Chakrabarti MK (2005). Involvement of phospholipase C in *Yersinia enterocolitica* heat stable enterotoxin (Y-STa) mediated rise in intracellular calcium level in rat intestinal epithelial cells. *Toxicon* **45**, 361–367.

Schroder M & Kaufman RJ (2005). The mammalian unfolded protein response. *Annu Rev Biochem* **74**, 739–789.

Sijen T, Fleenor J, Simmer F, Thijssen KL, Parrish S, Timmons L, Plasterk RH & Fire A (2001). On the role of RNA amplification in dsRNA-triggered gene silencing. *Cell* **107**, 465–476.

Soboloff J, Spassova MA, Hewavitharana T, He LP, Xu W, Johnstone LS, Dziadek MA & Gill DL (2006*a*). STIM2 is an inhibitor of STIM1-mediated store-operated Ca^{2+} entry. *Curr Biol* **16**, 1465–1470.

Soboloff J, Spassova MA, Tang XD, Hewavitharana T, Xu W & Gill DL (2006*b*). Orai1 and STIM reconstitute store-operated calcium channel function. *J Biol Chem* **281**, 20665.

Spassova MA, Soboloff J, He LP, Xu W, Dziadek MA & Gill DL (2006). STIM1 has a plasma membrane role in the activation of store-operated Ca^{2+} channels. *Proc Natl Acad Sci U S A* **103**, 4040–4045.

Tabara H, Sarkissian M, Kelly WG, Fleenor J, Grishok A, Timmons L, Fire A & Mello CC (1999). The *rde-1* gene, RNA interference, and transposon silencing in *C. elegans*. *Cell* **99**, 123–132.

Teramoto T & Iwasaki K (2006). Intestinal calcium waves coordinate a behavioral motor program in *C. elegans*. *Cell Calcium* **40**, 319–327.

Tian P, Estes MK, Hu Y, Ball JM, Zeng CQ & Schilling WP (1995). The rotavirus nonstructural glycoprotein NSP4 mobilizes Ca^{2+} from the endoplasmic reticulum. *J Virol* **69**, 5763–5772.

van Kuppeveld FJ, Hoenderop JG, Smeets RL, Willems PH, Dijkman HB, Galama JM & Melchers WJ (1997). Coxsackievirus protein 2B modifies endoplasmic reticulum membrane and plasma membrane permeability and facilitates virus release. *EMBO J* **16**, 3519–3532.

Venkatachalam K, van Rossum DB, Patterson RL, Ma HT & Gill DL (2002). The cellular and molecular basis of store-operated calcium entry. *Nat Cell Biol* **4**, E263–E272.

Vig M, Beck A, Billingsley JM, Lis A, Parvez S, Peinelt C, Koomoa DL, Soboloff J, Gill DL, Fleig A, Kinet JP & Penner R (2006*a*). CRACM1 multimers form the ion-selective pore of the CRAC channel. *Curr Biol* **16**, 2073–2079.

Vig M, Peinelt C, Beck A, Koomoa DL, Rabah D, Koblan-Huberson M, Kraft S, Turner H, Fleig A, Penner R & Kinet JP (2006*b*). CRACM1 is a plasma membrane protein essential for store-operated Ca^{2+} entry. *Science* **312**, 1220–1223.

Wu MM, Buchanan J, Luik RM & Lewis RS (2006). Ca^{2+} store depletion causes STIM1 to accumulate in ER regions closely associated with the plasma membrane. *J Cell Biol* **174**, 803–813.

Xu P, Lu J, Li ZYuX, Chen L & Xu T (2006). Aggregation of STIM1 underneath the plasma membrane induces clustering of Orai1. *Biochem Biophys Res Commun* **350**, 969–976.

Yan X, Xing J, Lorin-Nebel C, Estevez AY, Nehrke K, Lamitina T & Strange K (2006). Function of a STIM1 homologue in *C. elegans*: evidence that store-operated Ca^{2+} entry is not essential for oscillatory Ca^{2+} signaling and ER Ca^{2+} homeostasis. *J Gen Physiol* **128**, 443–459.

Yeromin AV, Roos J, Stauderman KA & Cahalan MD (2004). A store-operated calcium channel in *Drosophila* S2 cells. *J Gen Physiol* **123**, 167–182.

Yeromin AV, Zhang SL, Jiang WYuY, Safrina O & Cahalan MD (2006). Molecular identification of the CRAC channel by altered ion selectivity in a mutant of Orai. *Nature* **443**, 226–229.

Yin X, Gower NJ, Baylis HA & Strange K (2004). Inositol 1,4,5-trisphosphate signaling regulates rhythmic contractile activity of smooth muscle-like sheath cells in the nematode *Caenorhabditis elegans*. *Mol Biol Cell* **15**, 3938–3949.

Zhang SLYuY, Roos J, Kozak JA, Deerinck TJ, Ellisman MH, Stauderman KA & Cahalan MD (2005). STIM1 is a Ca^{2+} sensor that activates CRAC channels and migrates from the Ca^{2+} store to the plasma membrane. *Nature* **437**, 902–905.

Zhang SL, Yeromin AV, Zhang XHYuY, Safrina O, Penna A, Roos J, Stauderman KA & Cahalan MD (2006). Genome-wide RNAi screen of Ca^{2+} influx identifies genes that regulate Ca^{2+} release-activated Ca^{2+} channel activity. *Proc Natl Acad Sci U S A* **103**, 9357–9362.

Zweifach A & Lewis RS (1995*a*). Rapid inactivation of depletion-activated calcium current (I_{CRAC}) due to local calcium feedback. *J Gen Physiol* **105**, 209–226.

Zweifach A & Lewis RS (1995*b*). Slow calcium-dependent inactivation of depletion-activated calcium current. Store-dependent and -independent mechanisms. *J Biol Chem* **270**, 14445–14451.

Acknowledgements

This work was supported by NIH grants R01 GM74229 and R01 DK51610 to K.S. We thank Dr David Baillie for providing the BC10427 worm strain. Some *C. elegans* strains used in this work were provided by the *Caenorhabditis* Genetics Center (University of Minnesota, Minneapolis, MN). Confocal microscopy was performed in the Vanderbilt University Medical Center Cell Imaging Shared Resource, which is supported by NIH grants CA68485, DK20593, DK58404, HD15052, DK59637 and EY08126.